THE GENERATION AND SCAVENGING OF RADICALS VIA CERIUM AND NANOCERIA

by
ERIC GLENN HECKERT
B.S. University of Central Florida, 2004

A thesis submitted in partial fulfillment of the requirements
for the degree of Master of Science
in the Department of Molecular Biology and Microbiology
in the Burnett School of Biomedical Sciences
in the College of Medicine
at the university of Central Florida
Orlando, Florida

Fall Term
2007

ABSTRACT

Cerium is the most abundant of the rare earth metals, found on average at a level of 66 parts per million in the earth's crust. The unique redox properties of cerium and cerium oxide nanoparticles have led to its use in a wide variety of industrial and commercial uses such as oxygen sensors, fertilizers and as a catalyst to remove toxic gases in automobile exhaust. The use of cerium has also garnered interest in the nanotechnology field. Nanoceria has been generated in its oxide form as nanoparticles and nanorods. Recently, nanoceria has been shown to protect against oxidative stress in both animal and cell culture models. Although not fully understood, this observed protective effect of nanoceria is believed to be the result of recently identified SOD mimetic activity. Currently there is little understanding as to how nanoceria is capable of scavenging radicals or what properties makes nanoceria an effective SOD mimetic. Our data shows strong evidence that the oxidation state of nanoceria is directly related to its reported SOD mimetic activity. As such, future studies of nanoceria should be mindful of the oxidation state of nanoceria preparations as only nanoceria with a high concentration of cerium (III) have shown effective SOD mimetic activity. In addition to the characterization of nanoceria and its SOD mimetic activity, we have evidence that free cerium is capable of generating radicals and damaging DNA in vitro in the presence of hydrogen peroxide. These data strongly suggests that the rare earth inner-transition metal cerium is capable of generating hydroxyl radicals via a Fenton-like reaction. Based on these results the use of free cerium salts should be monitored to limit environmental exposure to cerium. Altogether our data would suggest that cerium by virtue of its unique redox chemistry is quite capable of accepting and donating electrons from its

surroundings. In its free form cerium is able to redox cycle easily and can generate radicals. However, paradoxically nanoceria may not easily redox cycle due to the bound lattice structure of the particle. The unique nature of nanoceria and cerium leads to a unique circumstance where nanoceria is a radical scavenger while free cerium generates radicals. As such, further investigation is needed to insure that leeching or cerium from nanoceria does not abrogate any potential benefit nanoceria may provide.

I would like to dedicate this thesis to my family for their support during this arduous endeavor.

TABLE OF CONTENTS

LIST OF FIGURES

LIST OF ABBREVIATIONS

ABTS	2,2'-azino-bis(3-ethylbenzthiazoline)-6-sulphonic acid
DEPMPO	5-(diethoxyphosphoryl)-5-methyl-1-pyrroline N-oxide
DPTA	Diethylene triamine pentaacetic acid
EDTA	Ethylenediaminetetraacetic acid
EPR	Electron Paramagnetic Resonance
Gpx	Glutathione peroxidase
RNS	Reactive Nitrogen Species
ROS	Reactive Oxygen Species
SOD	Superoxide Dismutase
XPS	X-ray Photoelectron Spectroscopy
Trx	Thioredoxin
UV	Ultra Violet

CHAPTER 1: INTRODUCTION

1.1 Nanotechnology

Nanotechnology is a broad and rapidly expanding field; it is generally defined as the development and manipulation of objects containing at least one dimension of 100 nm or less in size. Current research in nanotechnology has a number of relevant biomedical applications. These developments range from development of new drug delivery systems, contrasting agents like iron oxide nanoparticles for improved MRI imaging, fluorescent particles such as quantum dots for quantification and imaging of cells, development of new nano-based materials for medical treatments, among many other applications. (14)

The use of nanotechnology definitely holds the possibility of tackling many of the current issues in science and medicine today. However, with the increased use of nanotechnology there is also an increased risk of environmental exposure to heavy metals and other potentially toxic elements leeched from nanomaterials, as well as potential toxicity from the nanomaterials themselves. Already studies have shown that carbon nanotubes may be cytotoxic and there is currently debate as to whether other nanomaterials may be toxic as well (25, 27). As such nanotechnology, like all new areas in science, should be welcomed but also studied thoroughly to avoid any potentially unforeseen hazards.

1.2 Cerium

Cerium is a rare earth element belonging to the lanthanide series of the periodic table. Cerium is the most abundant of the rare earths, and is present at about 66 parts per million in the

earths crust or about 66 μg per gram of the earth crust by weight. Cerium is also present at approximately 1.2 nanograms per liter in ocean water (15). Cerium can exist in either the salt or oxide form and can cycle between the cerous, cerium (III), and ceric, cerium (IV), oxidation states. Cerium (IV) is often a yellow to red color while cerium (III) is usually white or colorless. Both oxidation states of cerium strongly absorb ultraviolet light and have two characteristic spectrophotometric absorbance peaks. The first peak is in the 230 to 260 nm range and corresponds to cerium (III) absorbance. The second peak absorbance occurs in the 300 to 400 nm range and corresponds to cerium (IV) absorbance (29).

Currently there is no known biological role for cerium. However, its present uses in industry, particularly in agriculture where cerium and other rare earth metals have been used to increase crop yields, could have the potential to environmentally expose large numbers of people to trace amounts of cerium (52). There are few published reports on the health effects from cerium exposure. However, recent literature has linked low levels of cerium with tropical cardiomyopathy endomyocardial fibrosis (24, 35). Previous reports suggested that low amounts of cerium caused an increase in fibroblast proliferation and that this increase in proliferation is likely in response to low levels of free radicals generated by redox cycling. Additional literature has linked rare earth metals with increase telomerase activity in human peripheral blood mononuclear cells (55). Altogether, it appears that trace amounts of cerium and other rare earth metals may be able to generate free radicals and cause oxidative stress in humans.

Currently there is a dearth of information on the pharmacokinetics of rare earth metals in humans. It could be assumed that rare earth metals are metabolized in a manner similar to other more common metals however, it is important to note that because rare earth elements are not

common in humans, or other organisms, cerium may not be sequestered as effectively as other more common metals such as iron. This could lead to retention of free cerium in humans and potentially cause chronic oxidative damage from trace amounts cerium due to the generation of free radicals.

1.3 Industrial uses for cerium

Bulk cerium oxide and free ceria salts have a number of different industrial roles. Free cerium is used in glass polishing, cracking in petroleum, fertilizers and oxygen sensors (52). Cerium oxide, by virtue of oxygen vacancy defects that occur naturally at the surface of the cerium oxide lattice, has a high oxygen storage capacity (45). As such, cerium oxide has found a number of industrial uses, especially in automotive exhausts where it has been shown to effectively reduce the amount of pollutants released from exhaust fumes (31, 41, 45).

1.4 Nanaoceria

Nanoceria has similar chemical and physical properties to bulk cerium, however, because nanoceria has many times the surface area of bulk cerium oxide and because there are surface oxygen vacancies present in nanoceria, nanoceria has the potential as a unique catalyst (48). Much of the unique chemistry involved with nanoceria is believed to be caused by the oxygen vacancy sites at the surface of the nanoceria lattice. As cerium oxide particles are formed, the roughly spherical shape of the cerium oxide particles causes the formation of vacancies or holes in the surface of the particle. These oxygen vacancies are characterized by cerium (III) atoms in the center of the vacancy surrounded by adjacent cerium (IV) atoms. The presence of cerium

(III) in nanoceria is unique to the center of the oxygen vacancy and the relatively high abundance of these vacancies in nanoceria is speculated to be responsible for the unique redox chemistry of nanoceria versus bulk cerium. (6, 32)

1.5 Current research with nanoceria

Current research with nanoceria is widely varied. Nanoceria research has involved its use in catalytic converters, as a scaffolding for carbonic anhydrase inhibitors, as an SOD mimetic, and as an oxygen sensor (17, 22, 31, 41). Additional work with nanoceria has involved the generation of differing nanosize and nanoshaped objects such as nanorods or nanoparticles that could potentially be used in electronics or for biomedical devices (23). Because of the unique redox properties of cerium oxide and other lanthanide based metals, nanoceria is being tested in both animal and cell culture models to determine the effects of oxidative stress on cells in the presence of nanoceria (22, 32, 42, 47). Current literature suggests that nanoceria may have some protective effects against oxidative stress, and that this observed protective effect of nanoceria may be due to the scavenging free radicals, although the exact mechanism behind this observed radical scavenging is unknown.

1.6 Fenton and Haber-Weiss chemistry

The univalent reduction of hydrogen peroxide was originally postulated by H.J.H. Fenton to explain the decomposition of hydrogen peroxide at low pH in the presence of iron (16). Iron, like other redox active metals such as copper, chromium, cobalt, vanadium and nickel, can

undergo a univalent reduction of hydrogen peroxide and generate a hydroxyl radical and a water molecule, see figure (1). This reaction is known as the Fenton reaction or Fenton chemistry and is the most common putative method by which hydroxyl radicals are formed in biology. Hydroxyl radicals ($HO^{\cdot}$), by virtue of the unpaired electron on the oxygen atom, are highly unstable with an estimated half life in the low nanosecond range (34). $HO^{\cdot}$ radicals are, due to their reactivity, very damaging to cells and are believed to be a major contributing factor in cellular senescence and aging.

$$Fe^{2+} + H_2O_2 + H^+ \longrightarrow Fe^{3+} + HO\cdot + H_2O$$

Fenton chemistry

Figure 1: Fenton reaction

Originally proposed by H.J.H. Fenton to explain the decomposition of peroxides in the presence of free iron. The iron dependant generation of hydroxyl radicals in the presence of hydrogen peroxide is considered a classical pathway for radical formation. Modified from Imlay et al. (1988).

In addition to the classical Fenton chemistry, other redox chemistry can occur with transition metals such as iron. The Haber-Weiss cycle, which builds upon Fenton chemistry, postulates that iron can behave as a catalyst in the breakdown of peroxides. The net result of the Haber-Weiss cycle is the breakdown of two hydrogen peroxide molecules to water and oxygen, see figure (2). Importantly, the Haber-Weiss cycle can occur regardless of the starting oxidation state of the metal. This is relevant because during Fenton reactions iron effectively acts as a reducing agent and is oxidized from Fe (II) to Fe (III) where, without the continued reduction of iron, the redox reaction would stop. However, in the Haber-Weiss cycle iron acts as a catalyst rather than a reactant in the presence of peroxides cycling from Fe (II) to Fe (III) and back again. Because of the potential redox cycling of metals, a small trace amount of free iron, or other redox active metal, could be able to generate a large amount of radicals from endogenous cellular peroxides.

However, it should be noted that the Haber-Weiss cycle is not the only possible pathway for metal dependent redox cycling in biology. In an isolated system with only iron and peroxides present the predominant pathway may be the Haber-Weiss cycle. However, previous literature has already shown that *in vivo* numerous things can reduce and oxidize metals (3, 37). Additionally, *in vitro* research has shown that iron and other metals are capable of causing DNA damage in the presence of peroxides (33). The nature of this reported DNA damage appears to be DNA nicking resulting from hydroxyl radicals. This strongly suggests that free metals, even in trace amounts, are likely to cause the formation of radicals that can damage cellular structures.

The potential hazards of free metals are further supported by the existence of iron storage proteins such as ferritin. Ferritin, as well as other metal chelating proteins like haemosiderin, are

highly effective metal sequestering molecules. A single ferritin molecule can store up to 4500 iron atoms (21). So effective are metal sequestering proteins, that some research has suggested that less than a single copper atom per cell is unsequestered during normal cellular functioning (38). Altogether, it is important to remember that Fenton chemistry represents only a simplified summary of the reaction between metals and peroxides and is not necessarily what may occur inside cells.

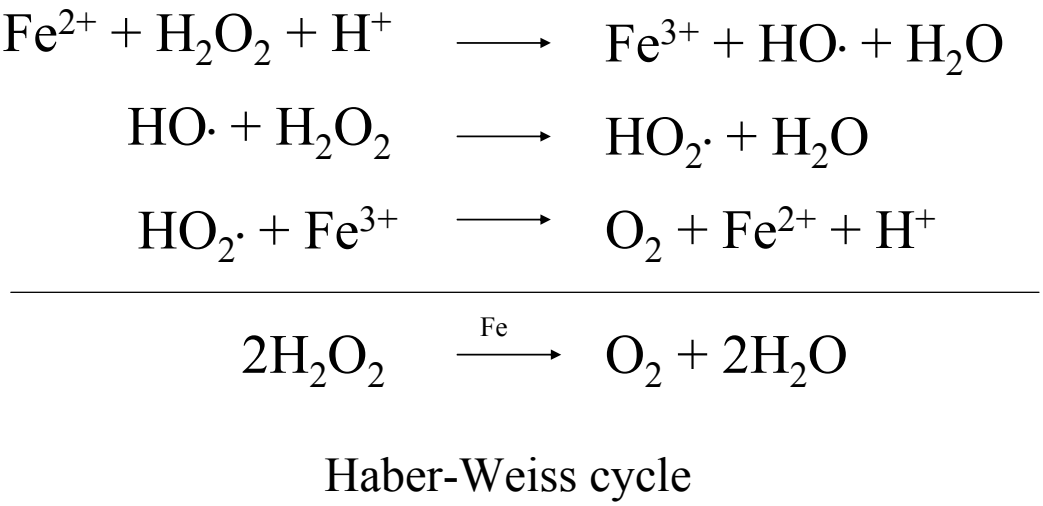

Haber-Weiss cycle

Figure 2: The Haber-Weiss reaction cycle

In this equation, which is an extension of the Fenton equation, iron acts in a manner similar to catalase and is converted to Fe(III) oxidation state and back to the Fe(II) oxidation state. This return to the original oxidation state allows a continued redox cycling of iron in the presence of peroxides. Modified from Imlay et al. (1988)

1.7 Sources of reactive oxygen species in cells

Although there are numerous sources of reactive oxygen species (ROS) within a cell, most evidence points to mitochondria as being the dominant source of endogenous ROS within a cell (12). An overwhelming majority of oxygen utilized within cells, approximately 99%, goes to the tetravalent reduction of oxygen to produce water via the mitochondrial electron transport chain (18). However, because iron sulfur clusters within the electron transport chain are somewhat prone to the direct one electron reduction of oxygen to superoxide, mitochondria can often generate large amounts of superoxide and other radical species. Although the exact amount of superoxide generated within mitochondria is unknown, estimates range from 0.1% to 2% of daily oxygen consumption generates superoxide (18). Although 2% is a relatively small amount of superoxide, without protective enzymes such as SOD even this amount would be more than enough to rapidly cause oxidative damage to cellular structures.

Although mitochondria may be responsible for the majority of ROS within eukaryotes it should be noted that many other cellular structures such as peroxisomes, lysosomes or the endoplasmic reticulum can also contribute to the oxidative damage that occurs within cells (53). In fact, even the mere presence of oxygen in cells is enough to generate ROS. This fact is evident because prokaryotes, which lack mitochondria still have cellular defenses against ROS and that if these defenses are removed these bacteria can no longer effectively survive (36).

In addition to mitochondria, and other cellular structures, immune cells are responsible for contributing to extracellular ROS and RNS levels. Perioxisomes within lymphocytes release nitric oxide and superoxide generated from inducible nitric oxide synthase (iNOS) and NADPH oxidase. Both superoxide and nitric oxide from lymphocytes are used to combat infections and

without these radicals lymphocytes would be highly ineffective at combating intracellular infections. However, due to the indirect nature of radical propagation lymphocytes undoubtedly cause collateral damage to surrounding uninfected tissue. As such, lymphocytes can be a significant source of damage to cells, particularly during an infection (39, 46).

Although ROS and RNS are responsible for significant amount of the cellular damage that occurs on a daily basis, removal of all ROS and RNS is not entirely possible. Other cells, such as endothelial cells in vasculature, use reactive nitrogen and reactive oxygen species as signaling molecules. Nitric oxide specifically is responsible for vasodilatation of the human vasculature and essential for proper physiological functioning within humans (8). Because of this complete removal of ROS and RNS from humans is neither achievable nor desired.

1.8 Pathologies associated with reactive oxygen species

Numerous diseases have been associated with the formation of reactive oxygen species, although the exact etiology of many pathologies are still unknown, most evidence suggests that oxidative stress is either the primary cause or an exacerbating agent in those diseases. One of the more recent discoveries in diseases related to ROS is the connection of ALS, as known as Lou Gehrig's disease, with a mutation in superoxide dismutase. Up to 20 % of Familial Amyotrophic Lateral Sclerosis (FALS) cases have been associated with gain of function mutations that occur in CuZn SOD (1, 26). Transgenic mice expressing mutations for mitochondrial SOD develop paralysis after several months while normal non-transgenic mice remained normal. Interestingly, because FALS is genetically dominant and because mitochondrial SOD retains catalytic activity, this evidence points to a gain of function mutation in mSOD that is resulting in neurotoxicity and

the development of FALS (26). Importantly, this gain of function mutation appears to be associated with a disregulation of copper used in SOD and that copper may be generating ROS in a Fenton like reaction.

Parkinson's disease is another ailment that has a strong connection with ROS. Neurodegeneration in Parkinson's appears to be associated with hydroxyl radical formation generated from an increase in free iron in the brain. Previous literature already has shown increased iron levels in the substantia nigra of Parkinson's patients and that iron chelators, such as clioquinol (CQ), desferoxamine (desferal) or antioxidants such vitamin E (alpha-tocopherol) have been successful in ameliorating the damage caused by increased iron levels (4, 19, 20). This research has led some research to postulate that Parkinson's may be caused by disregulation in metal metabolism and that the resulting neurotoxicity is a consequence of radicals generated by free metals.

Alzheimer's disease is another in a long list of neurodegenerative diseases associated with free radicals. Current literature is unclear as to the exact causative agent of Alzheimer's disease; however there is growing research to suggest that free metals and oxidative stress may play a role in exacerbating the disease. Previous literature has shown high levels of copper, zinc and iron in the amyloid plaques that are associated with Alzheimer's disease and that the amyloid-β peptide is which makes up these plaques are capable of binding free copper via its three N-terminal histidine residues. Interestingly, research has shown amyloid-β monomers to be relatively nontoxic and that the polymerization of these monomers via free radicals can lead to the formation of plaques that are characteristic in Alzheimer's disease. It appears that the amyloid-β peptide has the ability to generate oxidative stress both by the reduction of copper

available for antioxidant enzymes like SOD and by allowing amyloid-β bound copper and iron metals to redox cycle. Current research has also shown some success in treating Alzheimer's with the metal chelating compound clioquinol (CQ), further supporting the postulation that redox active metals play a role in Alzheimer's. Because of the complex nature of Alzheimer's disease it has been difficult to pinpoint the exact cause of the disease, however like many other diseases it appears that free metals and oxidative stress play a role in Alzheimer's disease (9, 56).

Cancer has many putative causes however; damage caused by free radicals has been associated with several forms of cancer. Much of the current research into cancer and free radical formation revolves around the alteration of DNA bases as well as the formation of double and single strand breaks in DNA. As there are many endogenous sources of ROS, DNA damage is likely caused by the cumulative effects of multiple sources that eventually lead to cancer. In addition to normal endogenous sources, there is a significant amount of evidence suggesting that cancer can be caused by high levels of redox active metals present in cells. Although ROS are not likely the only cause of cancer ROS is likely to play both a primary and secondary role in formation of different types of cancer (50, 51).

Cardiovascular disease is a vast and complicated pathology with numerous factors that may cause and exacerbate cardiovascular degeneration. Oxidative stress and tissue damage associated with ischemic reperfusion injury has a significant role in the pathology of vascular diseases (49). In addition to the damage caused by direct oxidative damage ROS also plays a role in the oxidation of lipoproteins and the formation of vascular plaques that lead to blood flow restriction and eventual heart attack or stroke. ROS can be both a causative agent in many forms

of cardiovascular disease and significant amount of research has shown that oxidative stress has been linked as an exacerbating agent in cardiovascular disease as well.

1.9 Cellular defenses against reactive oxygen species

Superoxide dismutase (SOD) is one of the first discovered and arguably most important enzymes in oxidative stress defense. SOD was originally discovered in 1939 by Mann and Keilin and named hemocuprein. Hemocuprein was later renamed to superoxide dismutase after its substrate and activity were characterized (28). SOD is responsible for protection of cells from superoxide. Superoxide results from the one electron reduction of molecular oxygen and has a number of putative cellular sources. As shown in figure (3), SOD converts $O_2^{\cdot -}$ to hydrogen peroxide and oxygen. Several different forms of SOD been have discovered including CuZn SOD, Mn SOD, and Fe SOD and, by virtue of their cellular locations, have been argued to play different corresponding roles in protection against ROS.

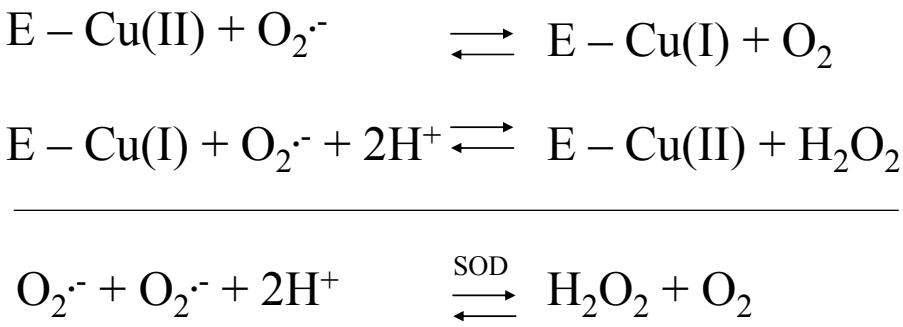

Figure 3: Proposed reaction mechanism of CuZn SOD

Although different forms of SOD contain different metals, nearly all SOD mechanisms center on the reduction and oxidation of a metal by superoxide and the formation of hydrogen peroxide. Modified from Liochev et al. (2003)

In addition to SOD several other enzymes play a critical role in cellular defense against ROS. Catalase, an enzyme responsible for the breakdown of hydrogen peroxide to molecular oxygen and water, works in conjunction with SOD to help convert superoxide to water and oxygen. Hydrogen peroxide, while more stable than superoxide, can be nearly as damaging to cellular macromolecules as superoxide. As mentioned previously hydrogen peroxide can interact with metals and generate hydroxyl radicals. Without catalase hydrogen peroxide levels would increase rapidly and generate large amounts of oxidative stress through Fenton chemistry.

Lastly, there are several other essential radical scavenging enzymes such as glutathione peroxidase (Gpx) and peroxiredoxins (Prx) that help in the removal of other cellular forms of radicals. Gpx and Prx differ from other previously mentioned radical scavengers in that they help to remove free radicals via sulfur bridges as opposed to metal oxidation and reduction. Gpx and Trx assist catalase in the reduction of different peroxides to alcohols. Thiol enzymes thereby help prevent oxidative damage by lowering endogenous peroxide levels. However, the thiol groups of Gpx are oxidized in the process of reducing peroxides and therefore require reduction by glutathione.

Trx is a protein that acts as an antioxidant in a manner similar to Gpx, however, Trx derives its reducing power from specifically from thioredoxin reductase (TrxR) and not glutathione. TrxR which derives its reducing power from an NADPH dependent reaction, is not an antioxidant per se, however it helps in preventing oxidative stress by reducing other essential peroxiredoxins via a cysteine thiol-disulfide exchange. As such, Trx and TrxR are often mentioned in tandem as they work together to help prevent oxidative damage. Trx and TrxR are essential for life and lack of cytosolic thioredoxin is embryonically lethal in mammals. In

addition to its role in defense against oxidative stress, thioredoxin also has a function in cell growth, apoptosis, and has chemokine and co-cytokine activites. Altogether SOD, catalase, Gpx, Prx, and Trx help play an orchestrated role in managing ROS levels and ameliorating ROS damage, without which aerobic life would be impossible (2).

CHAPTER 2: MATERIALS AND METHODS

2.1 Materials

Cerium (III) chloride heptahydrate, xanthine oxidase, and catalase were purchased from Sigma-Aldrich (St. Louis Missouri). Cerium sulfate, ferric chloride, ethylenediamine tetraacetic acid (EDTA), 1.2-diaminopropanetetraacetic acid (DPTA) and 4,5-dihyrdoxy-m-benzenedisulfonic (Tiron), hydrogen peroxide, tert-butyl peroxide and cytochrome C were from Acros Organics (Geel, Belgium). 2,2'-azinobis-(3-ethylbenzthiazoline-6-sulfonic acid), or ABTS was from Southern Biotech (Birmingham, Alabama). 6-hydroxy-2,5,7,8-tetramethyl-chroman-2 corboxlic acid (Trolox) was from EMD Bioscience (Darmstadt, Germany). Tris was obtained from MP Biomedicals (Solon, Ohio). The radical spin trap 5-(Diethoxyphosphoryl)-5-methyl-1-pyrroline-N-oxide (DEPMPO) was from Axxora, LLC (San Diego, California). Nanoceria preparations were prepared by Dr. Sudipta Seal's laboratory at the University of Central Florida (Orlando, Florida). All chemicals were of the highest grade available.

2.2 DNA nicking experiments

DNA damage was detected using supercoiled plasmid (pBR322) as a tool to measure the Fenton-like production of hydroxyl radicals. *E. coli* was harvested and plasmid (pBR322) was isolated and purified by alkaline lysis using a Strataprep EF plasmid kit (Stratagene, La Jolla, California). All reactions were performed in 100 μM Tris at pH 7.0. Ferric chloride was used as a standard for determining appropriate experimental conditions for Fenton chemistry monitered by nicking of supercoiled DNA. Excess (88 mM) hydrogen peroxide was added with either 20 μM ferric chloride or 100 μM cerium chloride. All reactions were incubated at 37° C for up to 60

minutes. To observe DNA damage at 10 minute intervals an excess of 10 mM EDTA was added to the reaction to stop radical formation from cerium or iron. The supercoiled DNA was resolved by electrophoresis on 0.7% agarose gels in Tris-Acetate-EDTA (TAE) buffer as previously described (44). Changes in plasmid migration are a result of DNA damage and can be directly assessed by agarose gel electrophoresis. Each lane of the gel was loaded with 100 ng of DNA run at 100 volts for 45 minutes and then soaked in TAE buffer containing 1 mg/100 ml ethidium bromide. Agarose gels were imaged using an Alphaimager 2200 UV transillumination (Alpha Innotech Corporation, San Leandro, California).

2.3 ABTS assay

ABTS radical formation was followed to assess the initial rate of free radical production from cerium in the presence of excess hydrogen peroxide. ABTS assays were performed as previously described in (7, 54). ABTS is converted to a stable radical cation ($ABTS^{+\cdot}$), see figure (4), upon the reaction with other radicals. ABTS creates a stable characteristic spectrum with a peak absorbance at 420 nm, see figure (5). Because of the relative stability of $ABTS^{+\cdot}$, the ABTS assay represents an effective and convenient way to measure radical formation spectrophotometrically. $ABTS^{+\cdot}$ was measured at 420 nm in 1 cm path length quartz cuvette at 25°C using an Agilent 8453 UV-visible spectrophotometer (Santa Clara, California). All reactions were performed in 100 μM Tris at pH 7.0. A full spectrum (200-900 nm) was recorded once per second for ten minutes. With the exception of temperature, the conditions were as similar as possible to the DNA nicking experiments. Several different concentrations of cerium chloride were tested in the presence of 88 mM hydrogen peroxide and 100 μM ABTS.

To assess the nature of radical formation by ceria several different scavengers were used in conjunction with the ABTS. The purpose of the radical scavengers was to competitively inhibit radical $ABTS^{+\cdot}$ formation as previously described (32). All radical scavengers (Tiron, Trolox, DEPMPO) were added prior to the addition of cerium chloride.

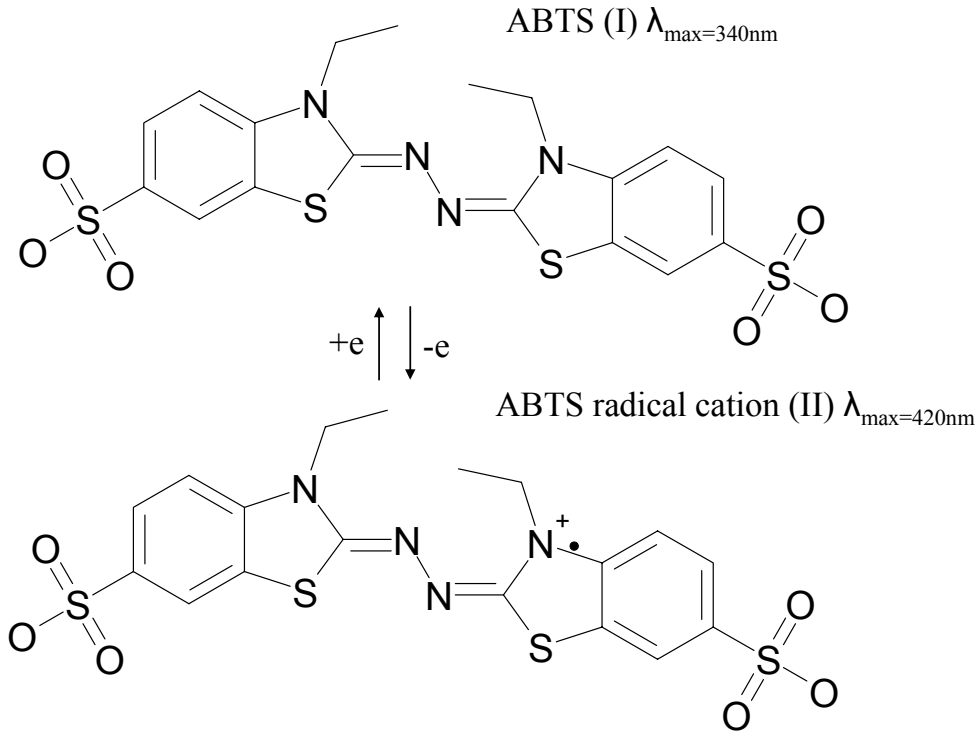

Figure 4: ABTS radical cation formation

Chemical structure of ABTS. ABTS becomes the cationic radical ($ABTS^{+\cdot}$) and generates a characteristic spectrum after a one electron reduction. ABTS is used as chromogen and is effective at measuring the initial rates of radical formation

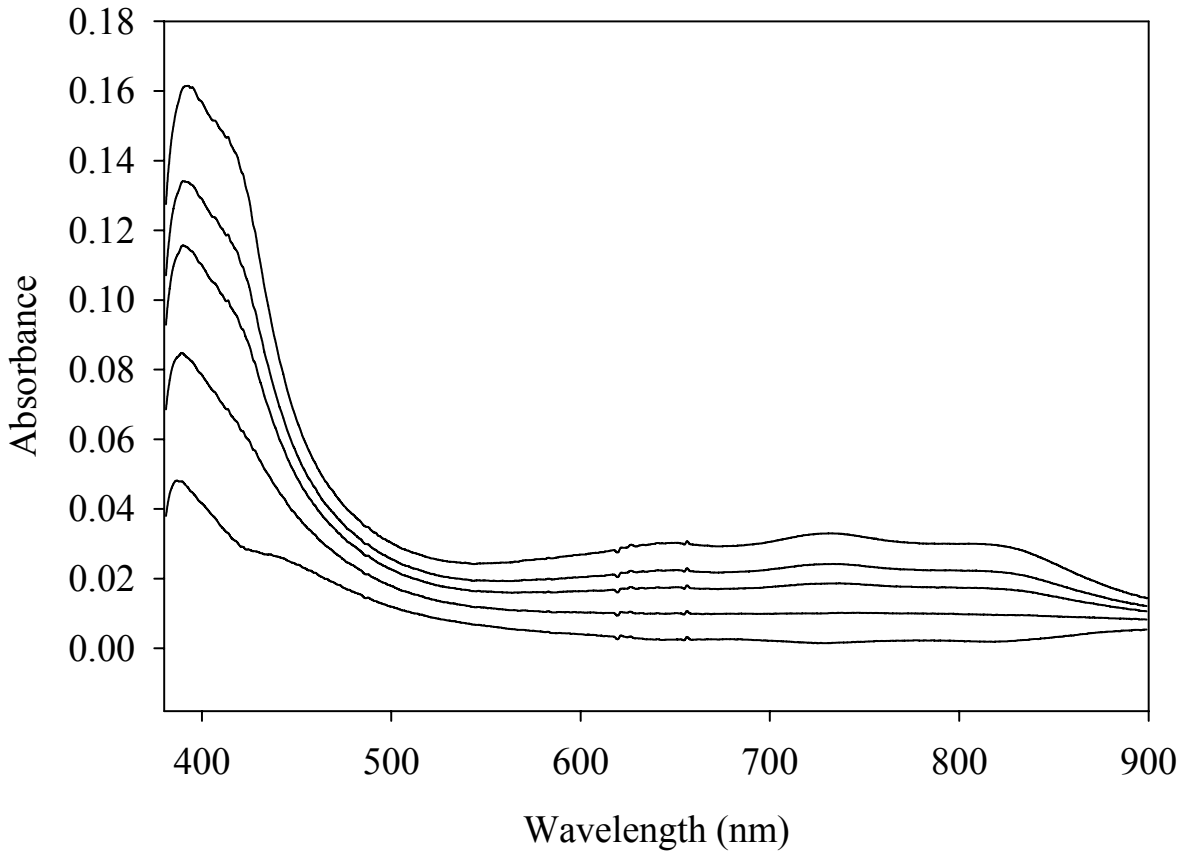

Figure 5: Characteristic spectrum of ABTS

Upon incubation of cerium chloride with hydrogen peroxide a characteristic $ABTS^{+\cdot}$ spectrum was formed. Each spectrum represents a one minute time point of $ABTS^{+\cdot}$ with 88 mM hydrogen peroxide and 100 μM cerium chloride.

2.4 EPR studies

EPR was use to identify oxygen radicals by using the spin trap DEPMPO as previously described (5). All reactions were buffered using 100 μM Tris buffer at pH 7.0. All reactions contained 100 mM hydrogen peroxide and 30 mM DEPMPO. Appropriate control reactions containing no cerium with or without hydrogen peroxide were performed; no detectable signal was generated. To test for radical formation from cerium in the presence of hydrogen peroxide, 1 mM Cerium (III) chloride heptahydrate ($CeCl_3 \cdot 7H_2O$) was added to solution containing hydrogen peroxide and DEPMPO. 5% DPTA was added to solution to prevent adventitious metals from contributing to radicals generated. EPR spectra were acquired using a Bruker Elexsys E580 EPR spectrometer. All spectra were collected in perpendicular mode using a Bruker model ER 4122SHQE super-high Q resonator. EPR settings used to detect radical formation were: 20 mW microwave power, 20.48 ms time constant, 81.92 conversion time, 0.5 G modulation amplitude, field set = 3514, sweep with = 100 G, number of scans 4.

2.5 Nanoceria UV-visible spectrum

Spectra for nanoceria were acquired using an Agilent 8453 UV-visible spectrophotometer (Santa Clara, California). An aliquot of nanoceria pretreated with 1.0 M H_2O_2 0.1.0 M H_2O_2 or control untreated ceria was diluted in water to 500 μM final concentration. Samples were blanked against water and then a spectrum of nanoceria was taken at various time points from 3 hours to16 days to measure the change in absorbance of nanoceria in the presence of hydrogen peroxide.

2.6 Determination of hydrogen peroxide concentration

An Amplex red peroxidase assay kit (A22188) from molecular probes (Eugene, OR) was used to detect hydrogen peroxide levels in nanoceria samples treated with peroxide at various time points from 3 hours to 16 days. Amplex red (10-acetyl-3,7-dihydroxyphenoxazine) has an excitation peak of 571 nm and an emission peak of 585 nm when converted to a fluorescent resorufin compound in the presence of horseradish peroxidase and hydrogen peroxide. After addition of hydrogen peroxide nanoceria samples were diluted to reduce the target level of hydrogen peroxide to 5 μM or less. Fluorescence measurements were taken in 96 well white microplates using a Varian Cary Eclipse spectrofluorometer (Varian, Palo Alto, CA). Fluorescence was measured using an excitation wavelength of 530 nm and an emission wavelength of 590 nm, the excitation and emission slit width was set at 5 nm and detection voltage was set at 400 V. Peroxide levels are reported as the level remaining with respect to starting concentration of 1.0 M or 0.1 M H_2O_2. A standard curve was generated using known amounts of hydrogen peroxide.

2.7 SOD mimetic assay

Reduction of ferricytochrome C was utilized to measure the SOD mimetic activity of nanoceria. Superoxide was generated by incubating 5 mM hypoxanthine and xanthine oxidase as previously described (13). Xanthine oxidase concentration was adjusted prior to each run to insure that control samples had an approximate reduction of ferricytochrome C of 0.025 absorbance units per minute. Each assay was run at room temperature for five minutes in a 96 well plate with a final total volume of 100 μL per sample. All reactions were buffered using 50

mM Tris buffer at pH 7.5. The rate of ferricytochrome C reduction was measured by following an increase in absorbance at 550 nm using a Spectramax 190 UV-visible spectrophotometer (Molecular Devices, Sunnyvale, CA). In order to determine the effect of hydrogen peroxide on the competitive inhibition of ferricytochrome C, nanoceria was treated with either 1.0 M or 100 mM hydrogen peroxide and aliquots were tested at 24 hour time points from 3 hours to 16 days. Nanoceria samples were diluted to 40 μM and assayed for SOD mimetic activity, as previously described (22). During each time point control samples and 40 μM untreated nanoceria samples were run in parallel. All samples included 2,000 units of catalase to eliminate any residual hydrogen peroxide that may react with either nanoceria or ferricytochrome C.

CHAPTER 3: SCAVENGING OF RADICALS WITH NANOCERIA-RESULTS AND DISSCUSSION

Recent studies suggest nanoceria can protect cells in culture against oxidative stress. However, the mechanism behind this protection is poorly understood and remains a gap in our knowledge today. Currently, the only proposed mechanism for this observed protective effect is the previously reported SOD mimetic activity. However, despite this insight, there is little in-depth knowledge as to how this reported SOD mimetic activity works, and how it may corresponds to the suggested protective effects of nanoceria. As such, exploration into the mechanism behind this SOD mimetic activity may both allow for a better understanding as to why nanoceria protects from oxidative stress as well as assist in the creation of more effective nanoceria particles.

3.1 EPR analysis of nanoceria in the presence of hypoxanthine/xanthine oxidase

In order to corroborate the previously reported SOD mimetic activity of nanoceria, electron paramagnetic resonance (EPR) was performed using hypoxanthine and xanthine oxidase to generate superoxide. EPR is considered one of the most reliable methods for the detection of radicals and its use is considered as a gold standard for identification of radical species. However, it is important to note that EPR conditions are not considered physiological and the concentrations and signals produced should only be used as a relative comparison for analysis.

To determine whether superoxide levels are affected by the presence of nanoceria, we generated superoxide using the hypoxanthine/xanthine oxidase system. We trapped this

superoxide radical using the spin trap DEPMPO as previously described (5, 11) In the presence of 500 μM nanoceria EPR signal intensity is significantly reduced (Figure 6). This strongly suggests that nanoceria can scavenge radicals and supports previous observations that nanoceria can act as a SOD mimetic. It is important to mention that hypoxanthine and xanthine oxidase almost exclusively generate superoxide as a radical in this system. This suggests that nanoceria is interacting directly with superoxide as asserted in prior literature, however, we cannot rule out the possibility that nanoceria can interact with other free radicals as superoxide is known to form other radical species through free radical propagation.

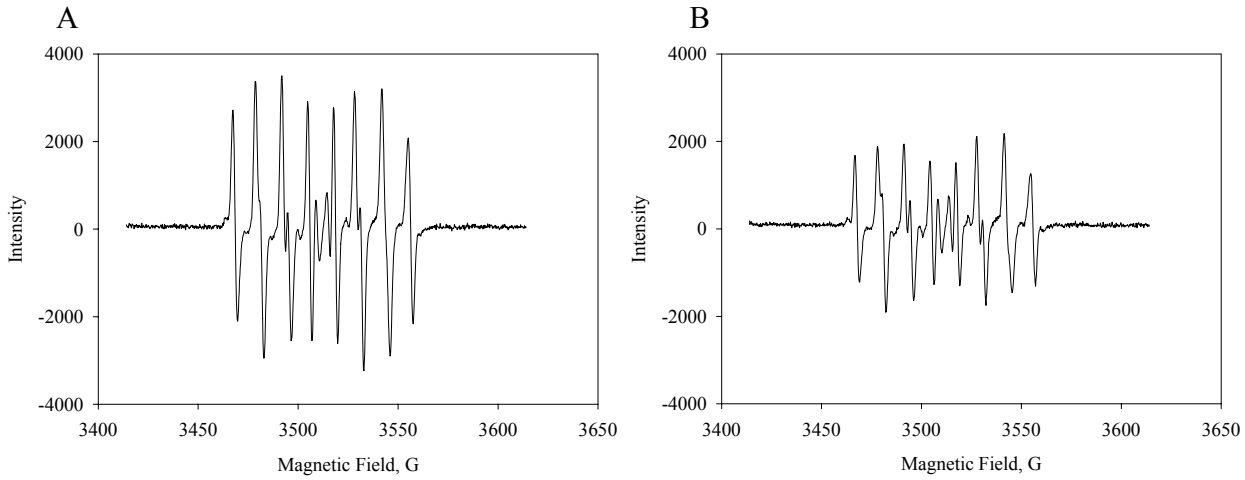

Figure 6: EPR spectra with and without nanoceria

(A) EPR spectrum represents superoxide DEPMPO adduct signal generated by hypoxanthine and xanthine oxidase. (B) EPR spectrum is identical to (A) with the exception of the addition of nanoceria. Both signals were generated using the same ESR settings and both signals were taken at the same time point during the course of the reaction.

3.2 Analysis of SOD mimetic activity of hydrogen peroxide treated nanoceria

Having established evidence that nanoceria can scavenge superoxide, the next step is to explore what conditions may effect nanoceria and its SOD mimetic activity. Previous studies

have shown that hydrogen peroxide can oxidize oxygen vacancies in nanoceria from cerium (III) to cerium (IV) (10). If oxidation state is a key component of nanoceria SOD activity, then hydrogen peroxide would be an effective means to probe this possibility. Therefore, we treated nanoceria with 1.0 M or 100 mM hydrogen peroxide to alter the oxidation state of surface vacancies and determined the oxidation state (UV-Visible) and SOD mimetic activity of nanoceria.

In order to assess SOD mimetic activity, nanoceria was tested using a ferricytochrome C assay. Experiments were performed at various time points after the addition of hydrogen peroxide and were conducted over a period of approximately two weeks. One molar hydrogen peroxide treated nanoceria lost all detectable SOD mimetic activity within 48 hours of addition of peroxide. Over the following 14 days, treated nanoceria regained nearly 100% of the original mimetic activity when compared to untreated samples, see figure (7). This clearly shows hydrogen peroxide is capable of temporarily inactivating nanoceria for this catalysis, however this inactivation is only transient and activity can return within several days.

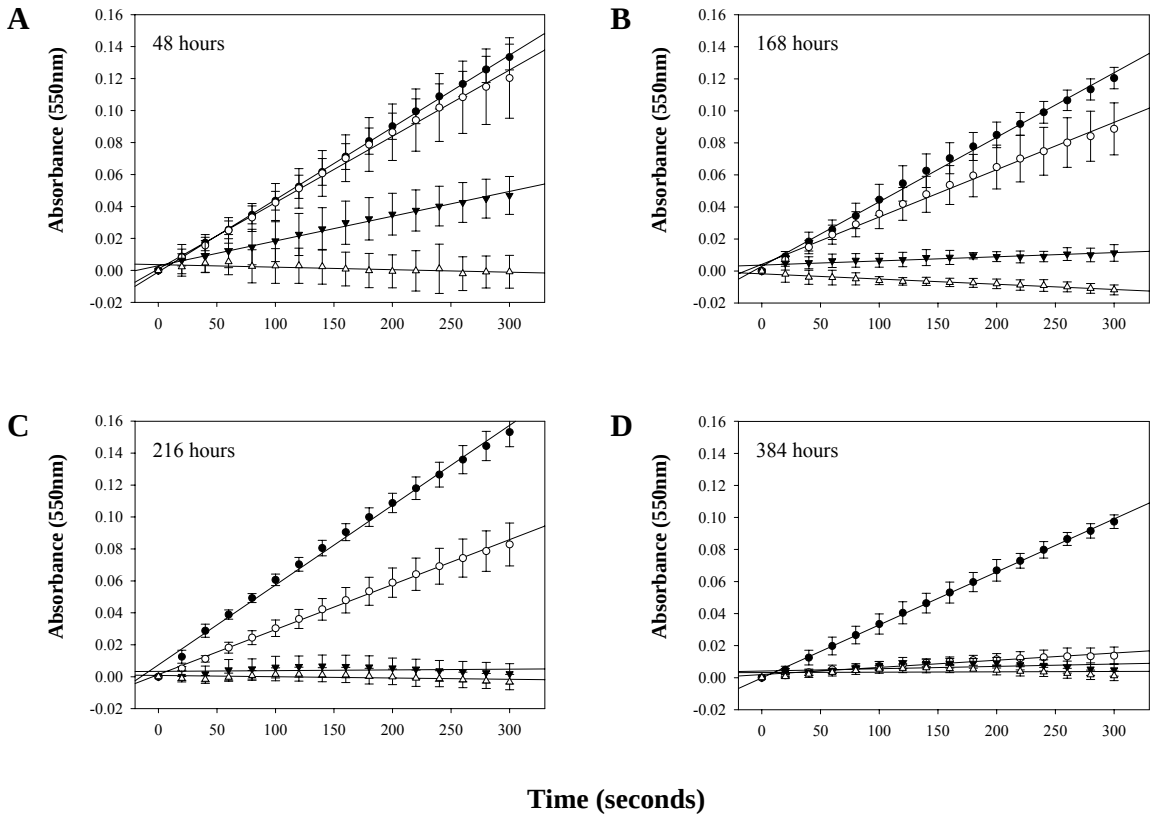

Figure 7: SOD mimetic activity in peroxide treated nanoceria

(A) competitive inhibition of ferricytochrome C reduction by superoxide after approximately 2 days, Filled circle: control, Open circle: 1.0 M H_2O_2 treated nanoceria, Filled triangle: 100 mM H_2O_2 treated nanoceria, Open triangle untreated nanoceria control. (B) 7days (C) 9 days (D) 16 days.

3.3 Determination of hydrogen peroxide levels using peroxidase assay

To evaluate what effect residual hydrogen peroxide levels may play on the SOD mimetic activity of nanoceria, an amplex red peroxidase kit was used determine hydrogen peroxide concentrations. All peroxide concentrations were measured using the same treated nanoceria used in ferricytochrome C assays and were conducted in conjunction with ferricytochrome C assay time points. Figure (8) clearly shows a drop in peroxide concentration over time, however when compared to ferricytochrome C assays in figure (7) there appears to be little correlation between absolute peroxide levels and the decrease in and subsequent return of SOD mimetic activity. This information suggests that it is the oxidation state of nanoceria from cerium (III) to cerium (IV) that is responsible for the resultant loss in SOD mimetic activity not any residual interfering peroxide.

It is also important to note that cerium oxide nanoparticles are not inactivated in ferricytochrome C assays merely by the presence of hydrogen peroxide as analysis of figure (7) and figure (8) clearly show that SOD activity returns well before all residual peroxide is gone. Furthermore, 2000 units of catalase are used in each ferricytochrome assay to remove any excess peroxide present during the experiment. Altogether this data suggests that the only relevant effect of hydrogen peroxide on nanoceria is to oxidize nanoceria from cerium (III) to cerium (IV) and that any residual hydrogen peroxide only serves to slow the rate at which nanoceria regains activity via changes in the surface chemistry.

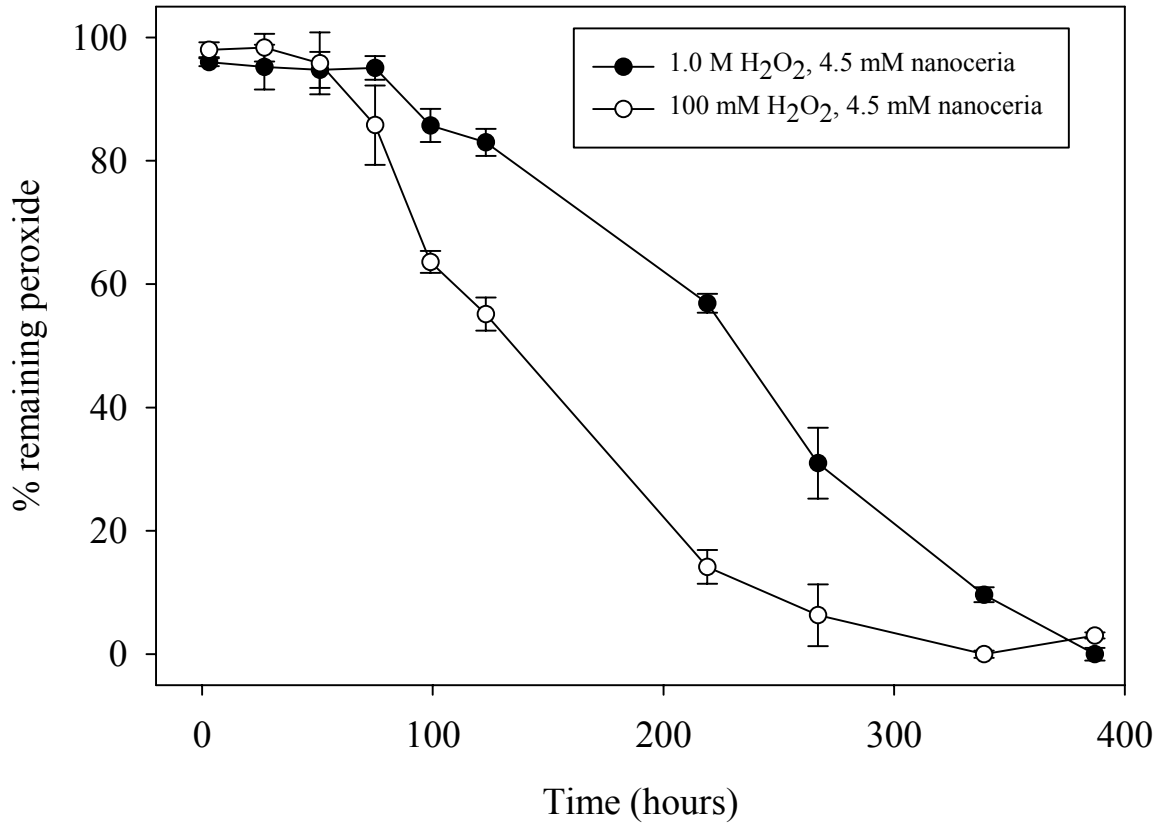

Figure 8: Hydrogen peroxide concentration in nanoceria samples

Hydrogen peroxide levels were measured using an amplex red assay. Peroxide levels were measured at set time points from 3 hours to approximately 384 hours.

3.4 Quantification of nanoceria oxidation state after treatment with hydrogen peroxide

In order to examine the oxidation state of nanoceria, spectrophotometric analysis was performed to help quantify cerium (III) and cerium (IV) concentrations. Oxidation of nanoceria should increase cerium (IV) concentrations and therefore should result in an increase in absorbance in the 300 to 400 nm range (29). The 230 to 260 nm spectral range, which corresponds to the cerium (III) concentration, should also show a corresponding decrease in absorbance after the addition of hydrogen peroxide. Unfortunately, hydrogen peroxide absorbs strongly in this region, and therefore this makes following any spectrophotometric changes in cerium (III) concentration impossible, see figure (9).

Figure 10A shows an increase in absorbance in the 300 to 400 nm range after the addition of 1.0 M hydrogen peroxide over a period of 387 hours (30). This observed increase in absorbance is congruent with both previous literature and our own data, and demonstrates that peroxides are capable of oxidizing nanoceria (43). Analysis of figure 7 and figure 10B shows that the changes in spectrophotometric absorbance over time matched inhibition in SOD mimetic activity and the return of SOD mimetic activity was accompanied by a corresponding drop in absorbance at 300-400 nm. This strongly suggests that the Cerium (III) to Cerium (IV) ratio is directly related to the reported SOD mimetic activity. This data also agrees with previous XPS analysis that showed nanoceria preparations containing high amounts of Cerium (IV) were ineffective in SOD mimetic assays (22).

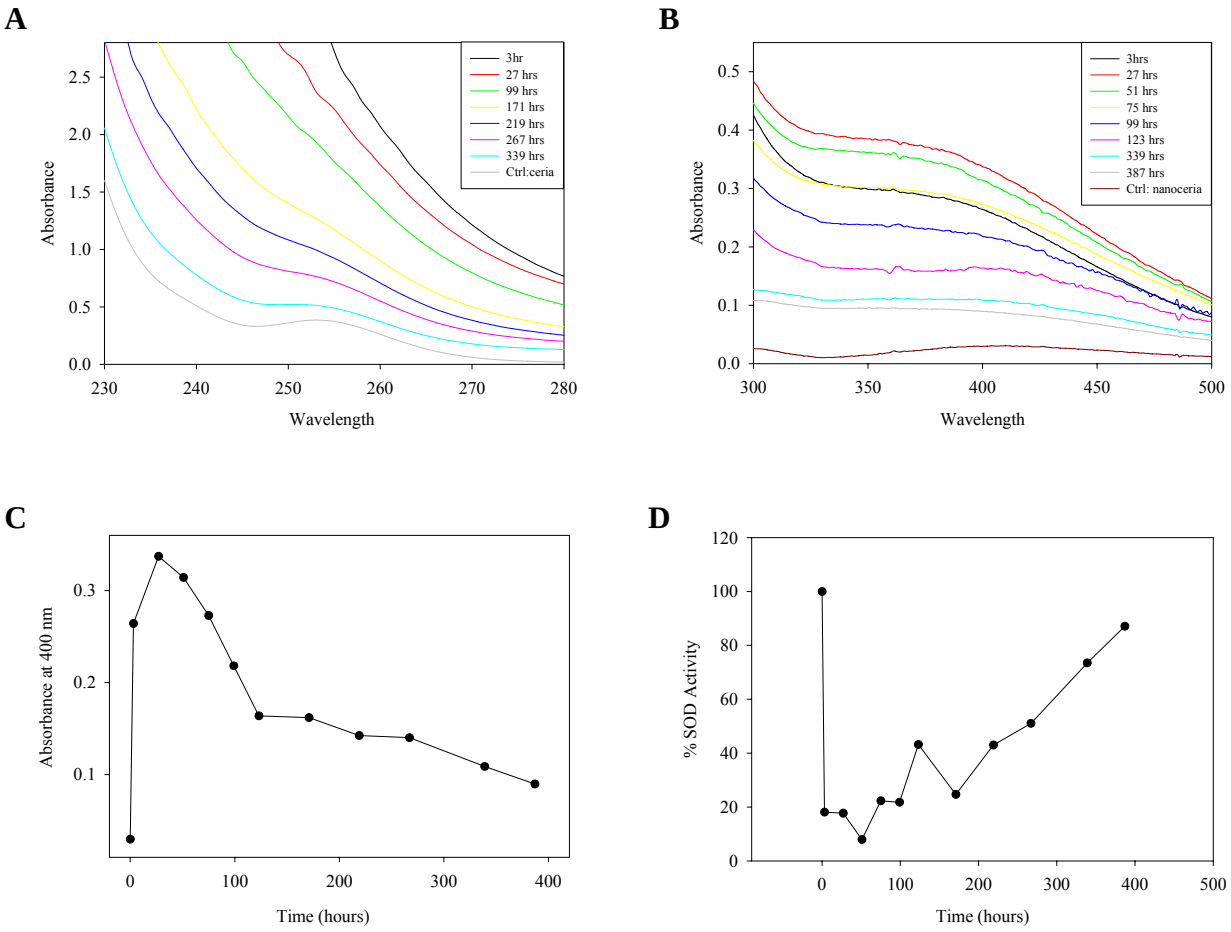

Figure 9: Spectrophotometric analysis of hydrogen peroxide treated nanoceria

UV-Vis spectra of nanoceria treated with 1.0 M hydrogen peroxide absorbance in the 400 nm range is due to cerium (IV). (A) Spectra of 300 to 400 nm range of hydrogen peroxide treated nanoceria at various time points. (B) UV-Vis spectra of nanoceria treated with 1.0 M hydrogen peroxide absorbance peaks at 255 nm are due to cerium (III) absorbance. Note that the peaks are obscured by the addition of hydrogen peroxide which absorbs strongly in the UV region. (C) Change in absorbance at 400 nm over time. (D) Relative change in SOD mimetic activity over time. Data was taken from a representative experiment that was subsequently reproduced.

3.5 Determination of nanoceria oxidation state after treatment with hydrogen peroxide and catalase

Because spectrophotometric determination of cerium (III) levels is impossible in the presence of hydrogen peroxide, an alternative method was required for analysis of cerium (III) concentrations. An additional sample of nanoceria was treated with 1.0 M hydrogen peroxide to alter surface cerium oxidation state. Nanoceria samples were incubated with hydrogen peroxide for two days to insure complete oxidation of test samples. After two days 4 units of catalase were added to the treated nanoceria samples. Catalase is an extremely effective enzyme capable of removing any residual peroxides rapidly. Near instantaneous removal of residual peroxides allow for both determination of SOD mimetic activity in the absence of hydrogen peroxide and further spectrophotometric examination of nanoceria. Figure 10 show the raw spectral data for nanoceria after the removal of hydrogen peroxide by catalase. Figure 11 clearly shows an inverse change in both cerium (III) and cerium (IV) over time, further demonstrating the capacity of hydrogen peroxide to oxide nanoceria and the capacity of nanoceria to return to the original cerium(III)/cerium(IV) ratio over time. If hydrogen peroxide levels were somehow responsible for SOD mimetic activity of nanoceria, the addition of catalase should cause activity should return immediately. SOD activity did return far sooner but did not return immediately upon removal of hydrogen peroxide by catalase (data not shown). This further suggests that oxidation state is responsible for the activity of nanoceria and helps to rule out the possibility that previous data may be tainted by artifacts generated by residual hydrogen peroxide.

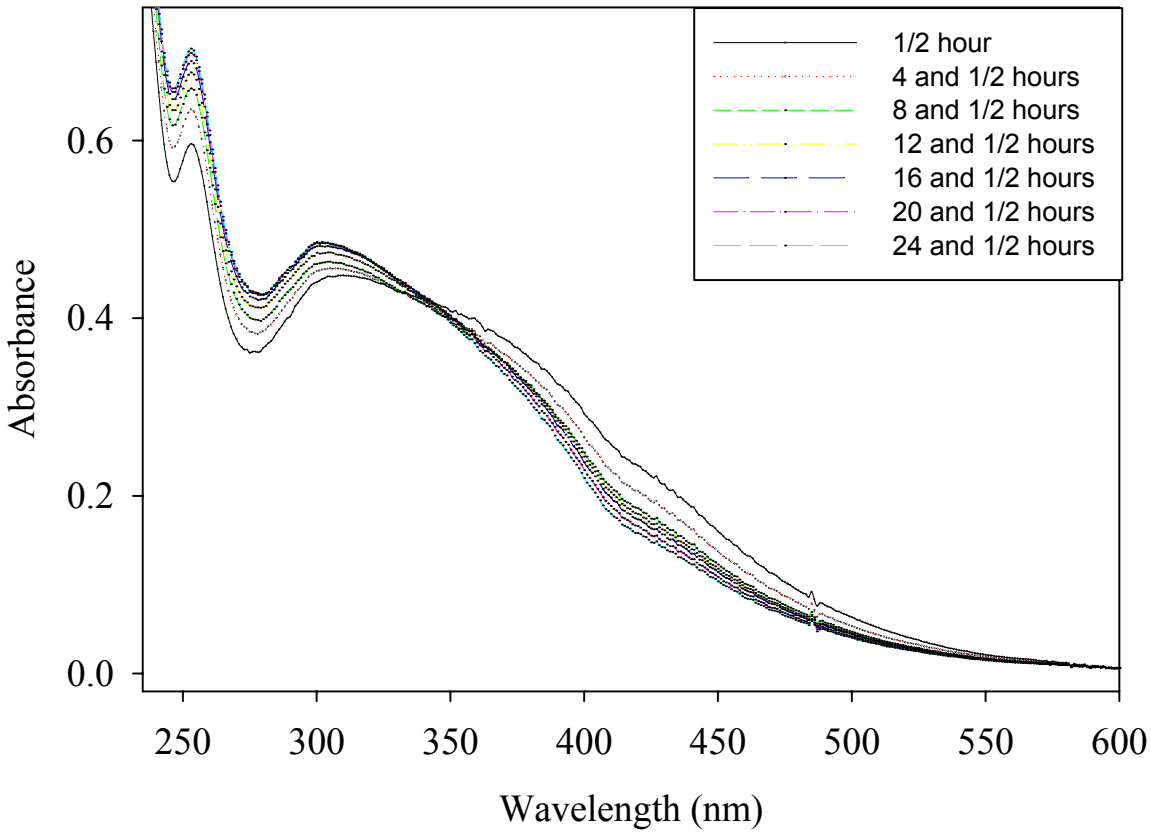

Figure 10: Change in nanoceria spectrum over time after addition of catalase

Spectrophotometric analysis of hydrogen peroxide treated nanoceria. Samples were treated with hydrogen peroxide for two days to insure oxidation of nanoceria then four units of catalase were added to remove excess peroxide. Note the peak at 252 nm corresponding to cerium (III) was previously obscured by excess hydrogen peroxide (Figure 9).

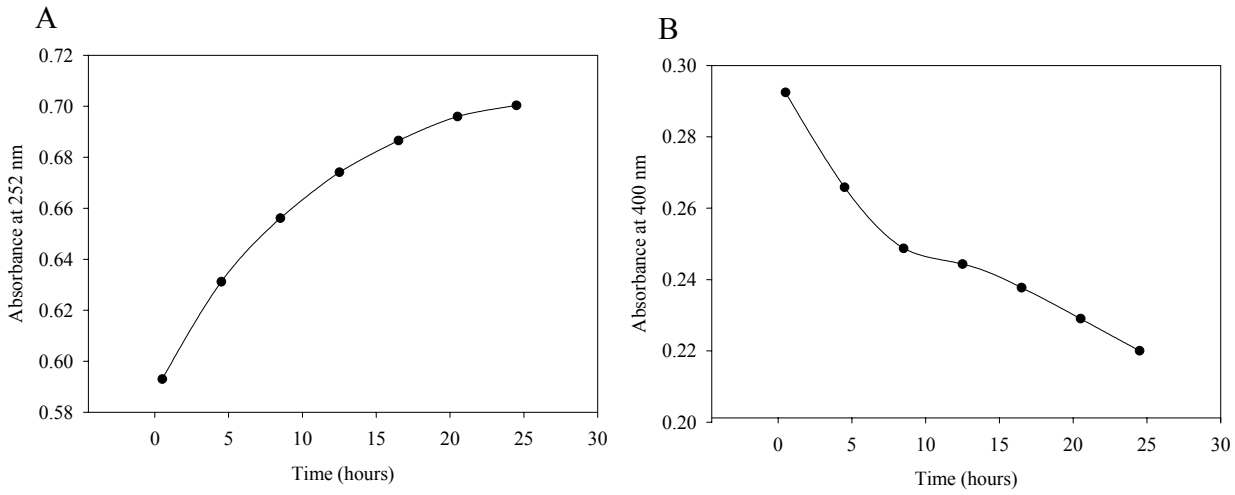

Figure 11: Change in cerium (III) and cerium (IV) over time

Spectrophotometric analysis of the rate of cerium (III) and cerium (IV) changes. (A) change in absorbance at 252 nm over time (B) change in absorbance at 400 nm over time. Note that cerium (III) corresponds to absorbance at 252 nm and cerium (IV) corresponds to absorbance at 400 nm.

A summary of the findings of this chapter are as follows:

1) UV-VIS data clearly shows that hydrogen peroxide causes a shift from cerium (III) to cerium (IV)

2) This shift correlates directly with a loss of SOD mimetic activity

3) The inactivation of nanoceria is only transient as nanoceria reacts with and breaks down peroxides and activity returns with time

4) Hydrogen peroxide levels, while important for oxidation of ceria, played no observable role in the SOD mimetic activity of nanoceria

5) Cerium (III) concentrations were inversely proportional to cerium (IV) concentrations and SOD mimetic activity returned concomitantly with the return of cerium (III)

6) The long term stability of nanoceria is unknown and free cerium may be leeched from nanoceria particles

Although nanoceria is capable of effectively removing excess hydrogen peroxide there are several differing possible methods for nanoceria to return to the cerium (III) oxidation state. Nanoceria will return to the original cerium (III) to cerium (IV) ratio in a few days depending upon concentration in the absence of any known reductants. This observed catalase activity, although rather weak in direct comparison to catalase, was still significant enough to allow for the decomposition of 1.0 M peroxide over the course of 2 weeks. Additionally, this catalase-like activity may help explain the regeneration of activity of nanoceria in the presence of peroxides.

Altogether, this data gives important insight into mechanism behind the SOD mimetic activity of nanoceria and makes a strong case for surface associated cerium (III) sites as the

active site of SOD mimetic activity. However, oxidation state is only one of several factors including size/surface area and oxygen vacancy sites that may be responsible for the effectiveness of nanoceria in both catalyzing the breakdown of peroxides and in SOD mimetic activity. Nanotechnology and bio-mimetics, (the generation of objects that mimic or improve upon the activity of biologically created enzymes or proteins) is a rapidly growing field of investigation. However if the introduction of artificially created nanomaterials such as nanoceria into biological systems is to be successful, further investigation of the underlying mechanism behind their effects is needed. Based on our data it is we conclude that previously the reported SOD mimetic activity can be inhibited with hydrogen peroxide and that this observed inhibition is a direct result of the oxidation of cerium (III) to cerium (IV). Therefore, it would be reasonable to recommend that any preparations of nanoceria used in future studies contain a significantly high ratio of cerium (III) to cerium (IV) and failure to include nanoceria with a higher cerium (III) to cerium (IV) ratio may result in erroneous results showing little or no cellular protection. Future studies to continue this as a molecular mechanism *in vivo* are needed.

CHAPTER 4: GENERATION OF FREE RADICALS FROM CERIUM-RESULTS AND DISSCUSSION

Many, but not all, transition metals can redox cycle under physiological conditions and generate free radicals through Fenton or Fenton-like reactions. Because of this, free metals in biology are rare and when found are often involved in disease. Cerium, an inner transition metal, has chemical and physical properties similar to other redox active metals. Because of these similarities, cerium is likely to behave in a manner analogous to other redox active metals; generating free radicals through the one electron reduction or oxidation of various substrates. The potential redox capacity of cerium may cause damage to cells through free radicals via Fenton-like chemistry. Therefore the redox cycling of cerium deserves investigation to further understand and avoid any possible hazards.

4.1 Plasmid relaxation by Fenton-like chemistry

In order to examine whether cerium can generate free radicals in the presence of peroxides, DNA nicking experiments were performed. If cerium generates radicals in the presence of hydrogen peroxide supercoiled plasmid DNA should be nicked creating open circular DNA. Figure (12) shows a dose and time dependent nicking of DNA with cerium and hydrogen peroxide. The addition of 100 μM cerium generated similar levels of DNA damage as 20 μM iron. It is important to note that, while the cerium concentrations are 5 times higher than the levels of iron used to generate similar levels of DNA damage, the difference in concentrations between iron and cerium is less than one order of magnitude. The addition of 5

μM DPTA (a chelating agent) did not significantly reduce the DNA damage caused by cerium in the presence of hydrogen peroxide and the addition of 100 μM cerium without hydrogen peroxide failed to generate any observable DNA damage (data not shown). The data argues that trace levels of other metals in the cerium sample are not responsible for this damage. Equal molar DTPA did effectively eliminate DNA damage indicating cerium salts are efficiently chelated by DTPA (data not shown).

Interestingly, cerium may be capable of generating radicals from other peroxides other than hydrogen peroxide, as the addition of tert-butyl peroxide and cerium is also capable of generating DNA damage with a similar concentration of peroxide. The simplicity of DNA nicking experiments assures a low likelihood of artifacts and helps to establish strong evidence for the formation of radicals. Our data clearly shows the formation of free radicals from cerium in the presence of peroxides and establishes that cerium is capable of Fenton-like chemistry.

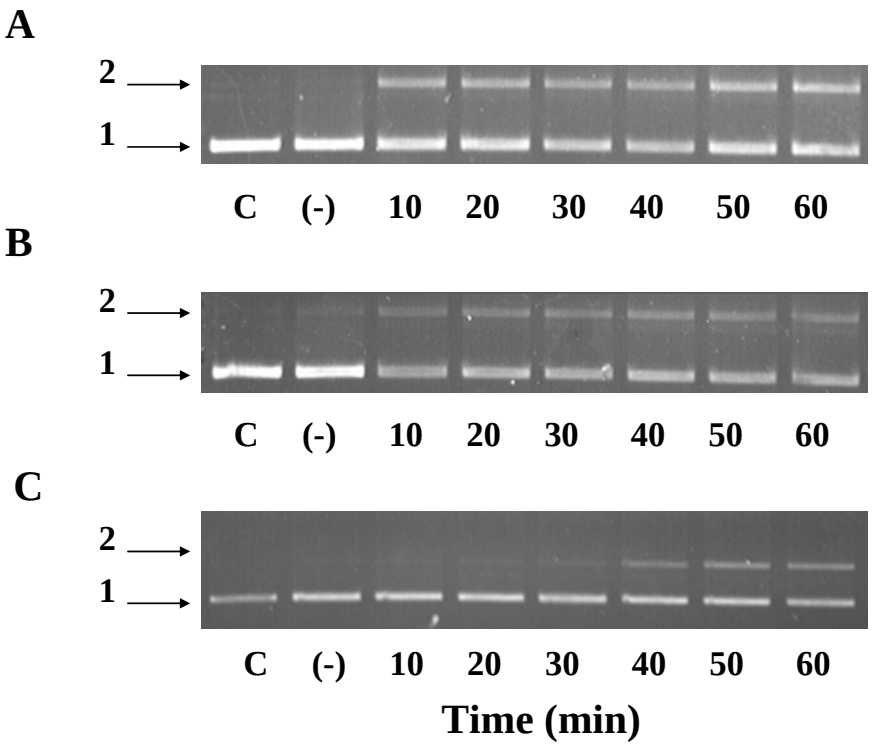

Figure 12: DNA nicking caused by a Fenton-like reaction of cerium with peroxides

Form 1 (indicated by arrows) is supercoiled plasmid and Form 2 is nicked supercoiled plasmid DNA. Aliquots from reaction were taken every ten minutes for one hour. At each time point the reaction was stopped using 10 mM EDTA and DNA was analyzed using 0.7% agarose gel electrophoresis. C: represents untreated DNA, (-) represents DNA with 88 mM hydrogen peroxide incubated for 60 minutes with no added cerium. (A) ferric chloride 20 μM control with 88 mM H_2O_2, (B) Cerium chloride at 100 μM with 88 mM hydrogen peroxide, (C) Cerium chloride 100 μM with 68 mM tert-butyl peroxide.

4.2 Formation of free radicals by cerium in the presence of peroxides

To further explore our initial hypothesis that cerium can generate free radicals in the presence of peroxides several different spectrophotometric assays were used. Initial experiments with cerium and hydrogen peroxide were performed with 2,2'-azino-bis(3-ethylbenzthiazoline)-6-sulphonic acid (ABTS). ABTS allows for a convenient and continuous spectrophotometric measurement of any potential radicals formed. ABTS creates a characteristic cation radical ($ABTS^{\cdot+}$) that can be easily followed and can allow for measurement of the initial rate of radical formation. It is important to note that ABTS is not a direct measurement of radical formation by cerium and therefore is may be prone to spurious results due redox chemistry. However, previously performed DNA nicking experiments have unequivocally shown free radical formation from cerium and as such, ABTS is a useful tool to explore the kinetics and behavior of radical formation from cerium.

Figure (13), clearly shows a dose dependent increase in $ABTS^{\cdot+}$ formation with cerium in the presence of peroxides. Although not linear with respect to concentration, the increased rate of $ABTS^{\cdot+}$ formation in the presence of increasing amounts of cerium strongly supports our previous experiments that cerium can generate free radicals in a manner analogous to other redox metals.

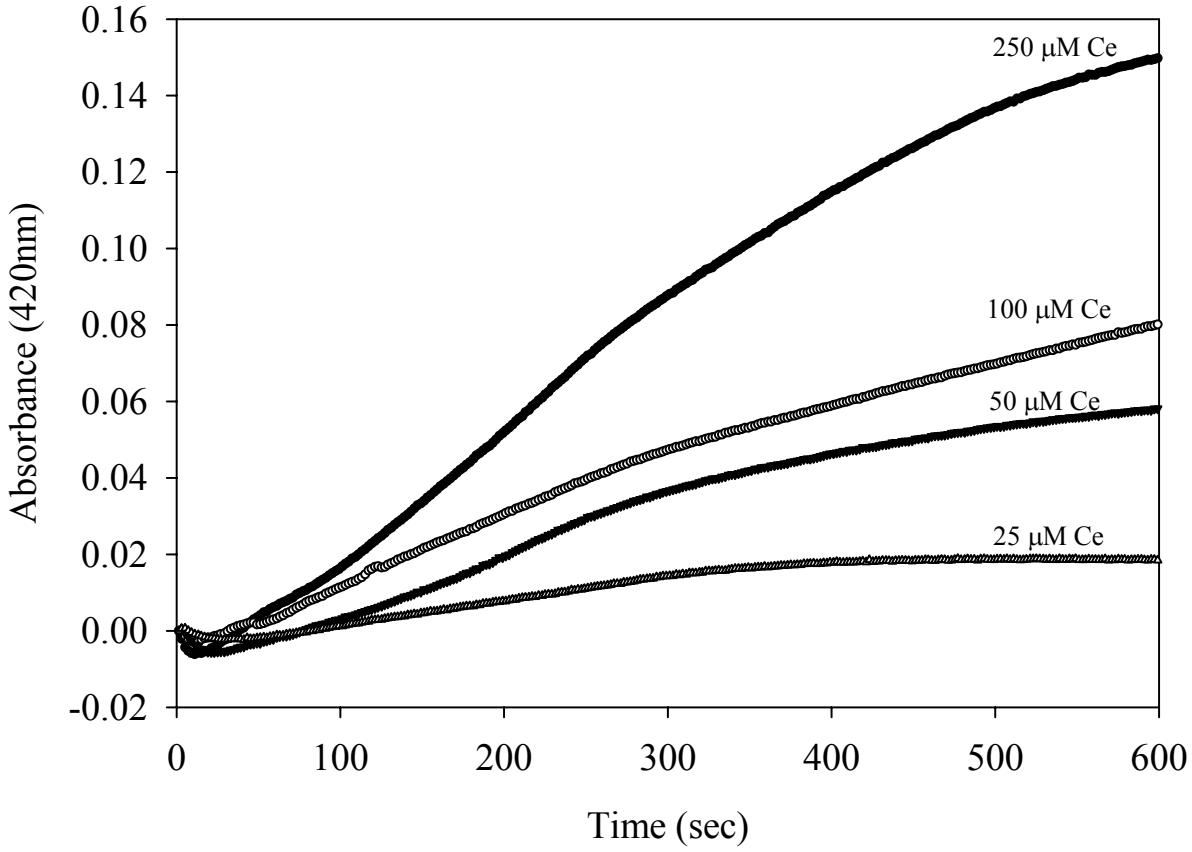

Figure 13: Initial rate of radical production from cerium in the presence of hydrogen peroxide

Over ten minute period $ABTS^{\cdot+}$ is followed in the presence of varying concentrations of cerium chloride and 88 mM hydrogen peroxide. $ABTS^{\cdot+}$ formation was monitored spectrophotometrically by measuring the increase in absorbance at 420 nm.

4.3 Scavenging of radicals produced from Fenton-like chemistry using DEPMPO

To further explore the nature of radical formation of cerium with peroxides, several different radical scavengers were added and the rate of $ABTS^{\cdot+}$ radical formation was measured. The first reagent used in ABTS assays was 5-(diethoxyphosphoryl)-5-methyl-1-pyrroline N-oxide (DEPMPO). DEPMPO is classified as spin trap and is commonly used in EPR experiments. The use of DEPMPO in EPR is due to the ability of DEPMPO to react with radicals including superoxide and hydroxyl radicals, and to insure the generation of a stable radical ion signal for analysis. The addition of DEPMPO reduced the rate $ABTS^{\cdot+}$ formation in a dose dependent manner, see figure (14). The inhibition of $ABTS^{\cdot+}$ radical formation with a spin trap is particularly important as this strongly suggests that the formation of an $ABTS^{\cdot+}$ radical signal is the result radical formation via Fenton-like chemistry from cerium and not an artifactual result of a direct chemical reaction between ABTS and cerium. However since DEPMPO can trap both superoxide and hydroxyl radical it is impossible to determine exactly which radicals may be formed.

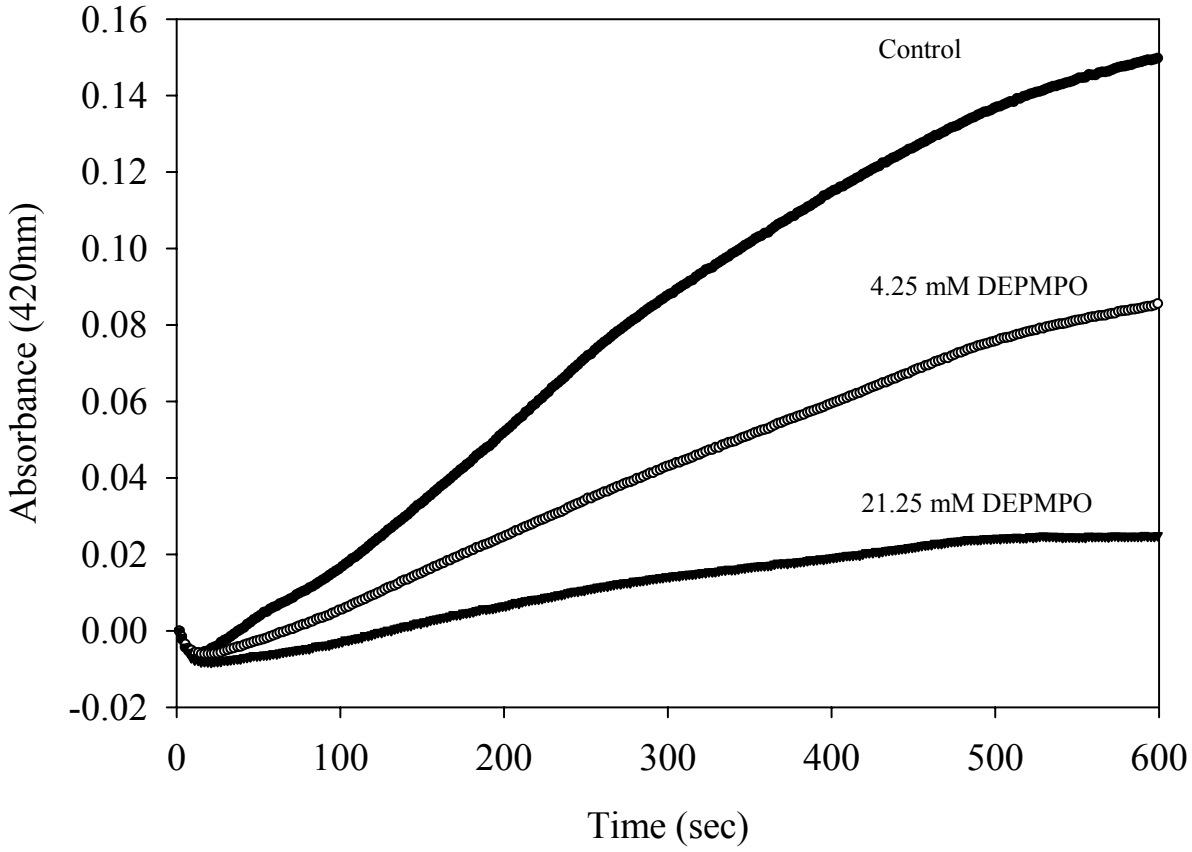

Figure 14: Radical scavenging by DEPMPO in the presence of cerium and hydrogen peroxide

Spin trap DEPMPO inhibits $ABTS^{\cdot+}$ formation in the presence of 100 μM cerium chloride and 88 mM hydrogen peroxide. Inhibition of radical formation is concentration dependent.

4.4 Scavenging of radicals produced from Fenton-like chemistry using Trolox

In addition to spin trap reagents, we also examined the effect of adding antioxidants (radical scavengers) in the ABTS assay. The first antioxidant used was Trolox, a water soluble analogue of vitamin E. Trolox is an antioxidant that has been shown to prevent lipid peroxidation *in vivo*. Previous publications have shown vitamin E is effective at preventing oxidative damage from iron and other redox active metals *in vivo* and *in vitro*, presumably by reacting with hydroxyl radicals or downstream radical intermediates (40). Figure (14) clearly demonstrates that Trolox can inhibit $ABTS^{\cdot+}$ formation in a dose dependent manner. However, because Trolox also is a nonspecific radical scavenger, these assays confirm previous DEPMPO experiments but do not give any detailed information into the type of radicals that may be formed.

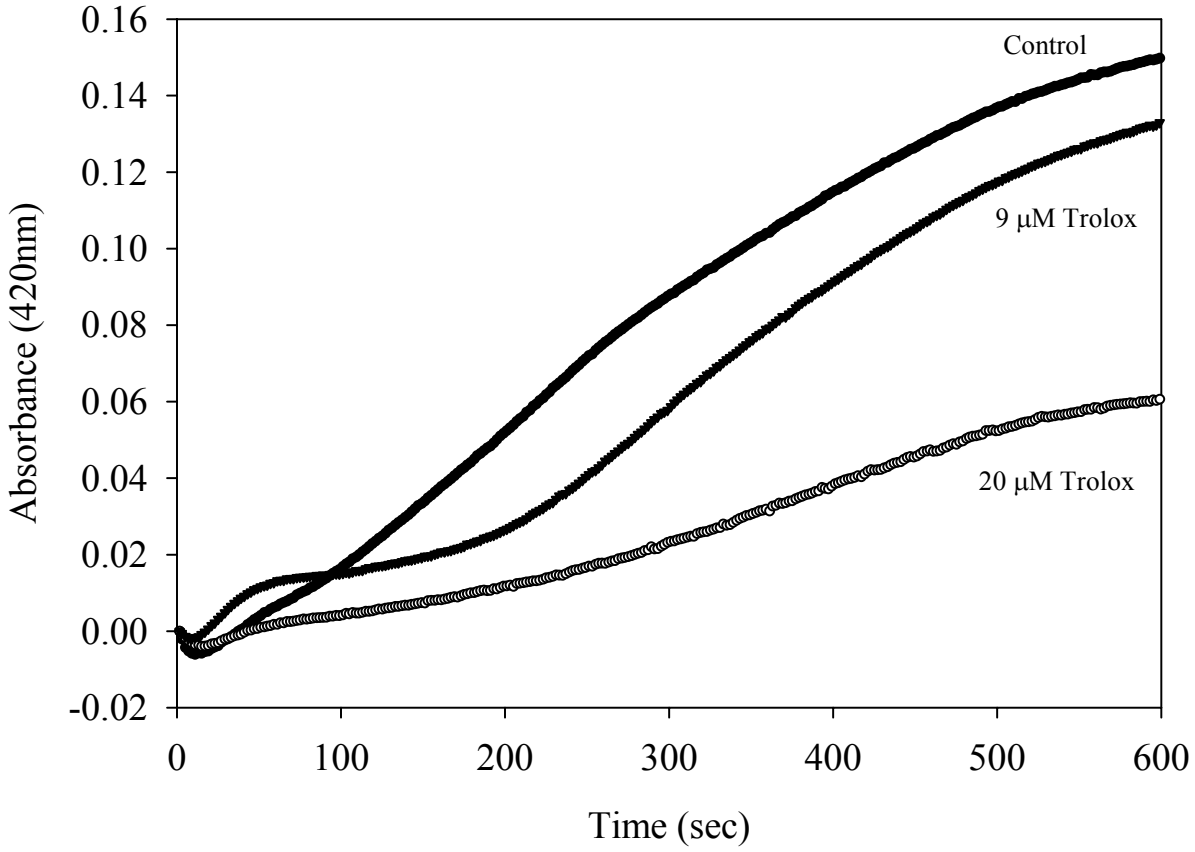

Figure 15: Radical scavenging by Trolox in the presence of cerium and hydrogen peroxide

Addition of varying concentrations of a Trolox, an analogue of vitamin E, prevents the formation of $ABTS^{\cdot+}$ by the Fenton-like reactions catalyzed by cerium.

4.5 Scavenging of radicals produced from Fenton-like chemistry using Tiron

To further confirm previous experiments and examine the type or types of radicals that may be generated from cerium dependent Fenton chemistry, Tiron was added with cerium and hydrogen peroxide and the resultant $ABTS^{\cdot+}$ radical signal was measured. Tiron, also classified as a spin trap, has been reported to exhibit SOD mimetic activity (5). Tiron, like Trolox, also inhibited $ABTS^{\cdot+}$ formation (Figure15) . The reported activity of Tiron as an SOD mimetic is important because the inhibition of $ABTS^{\cdot+}$ formation by Tiron suggests that cerium redox cycling may be generating superoxide. While this may be a deviation from traditional Fenton chemistry, prior literature has already confirmed the generation of both superoxide and hydroxyl radicals from chromium redox cycling (5, 51). Therefore the possible generation of superoxide by cerium does not necessarily rule out Fenton-like chemistry as the cause of free radical formation by cerium.

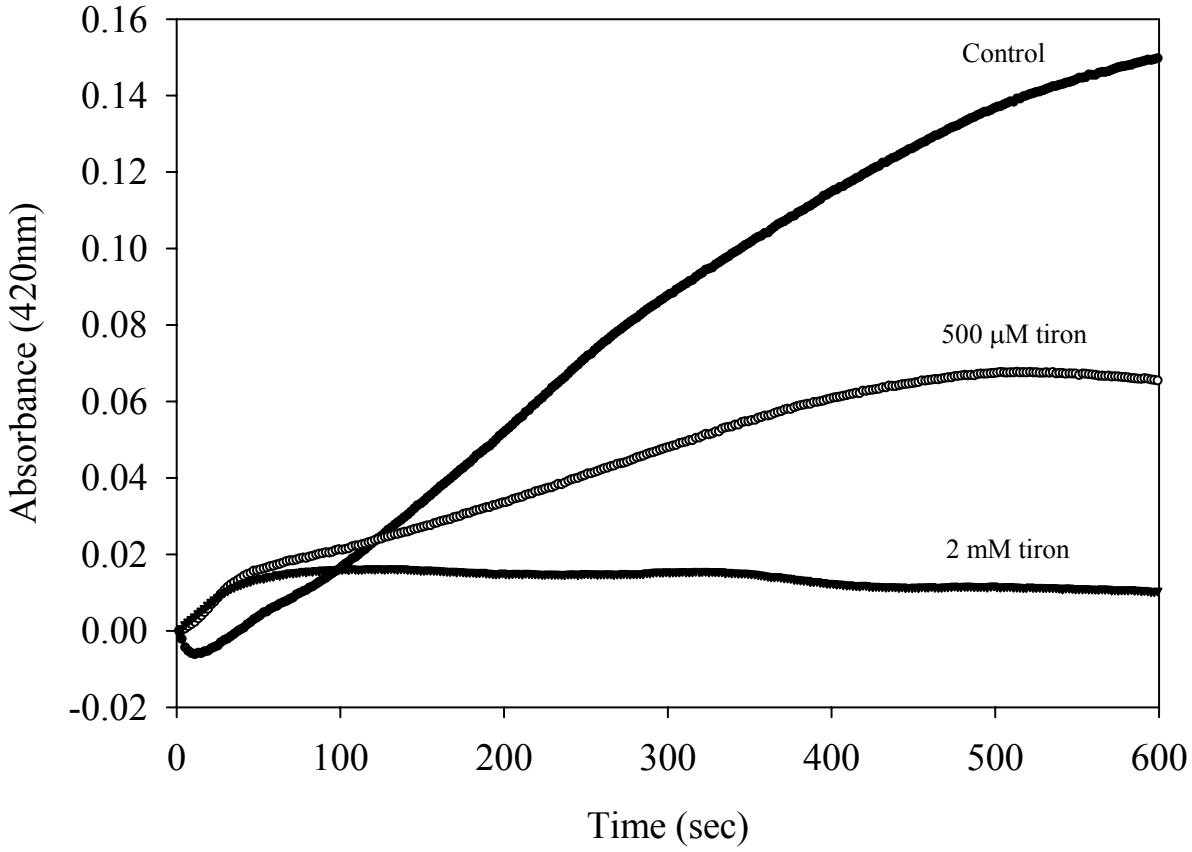

Figure 16: Radical scavenging by Tiron suggests superoxide formation

Addition of increasing concentrations of Tiron, a radical scavenger with SOD mimetic activity, prevents the formation of $ABTS^{\cdot+}$ radical cation formation.

4.6 EPR analysis of radicals formed from free cerium in the presence of hydrogen peroxide

To further investigate the exact nature of the radical formed, electron paramagnetic resonance was performed using the spin trap DEPMPO in the presence of cerium and hydrogen peroxide. It has been previously shown that DEPMPO can trap both superoxide and hydroxyl radicals, and that there species can be differentiated and quantified in mixtures (5, 11).The EPR data, figure (17), shows a strong radical signal in the presence of ceria and hydrogen peroxide. Analysis of the EPR spectra shows a mixture of approximately 50% superoxide and 50% hydroxyl radical. Addition of 5% DPTA, a chelating agent derived from EDTA, did not significantly effect or inhibit the formation of an EPR radical signal. This is important because this largely rules out the possibility of adventitious metal contamination as the source for radical generation.

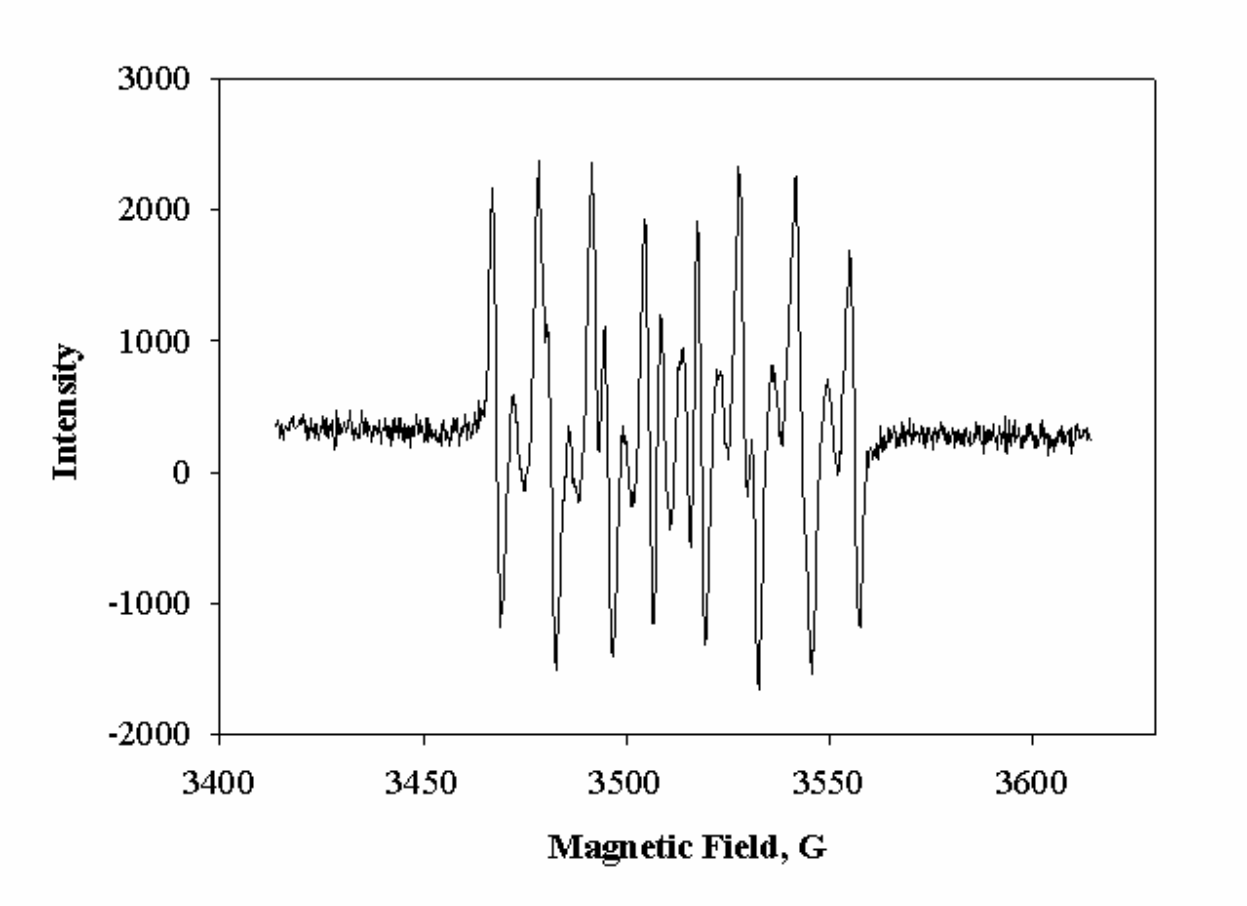

Figure 17: EPR spectrum of cerium in the presence of hydrogen peroxide

EPR spectrum of trapped DEPMPO radical adducts formed in the presence of 100 μM cerium chloride, and 100 mM hydrogen peroxide and 5 μM DTPA to chelate any adventitious metals in the cerium solution.

A summary of the findings of this chapter are as follows:

1) DNA nicking experiments strongly suggests that ceria can redox cycle in the presence of peroxides

2) ABTS analysis shows $ABTS^{+\cdot}$ formation is directly proportional to cerium concentration

3) The use of different spin traps and antioxidants suggest that the type of radical produced is likely a combination of both superoxide and hydroxyl radicals

4) EPR experiments confirm the formation of radicals with cerium and the presence of both superoxide and hydroxyl radicals

Although, far less prevalent than other metals in nature, the relative abundance and use of ceria in industry strongly suggest that environmental contact with cerium and humans is and will continue to occur. Because there is no known biological role for cerium, metal binding proteins like ferritin may not chelate cerium efficiently. Based on these results future studies should focus on the toxicity of cerium salts and their ability to cause oxidative stress. It is possible that cerium maybe leached from nanoceria and be capable of redox cycling and generating radicals. Altogether our data shows strong evidence for the generation of radicals from cerium in the presence of peroxides, although further studies may be needed to explore the exact nature and conditions of radical formation with cerium. Any future use of cerium salts or nanoceria in industry or medicine should proceed cautiously to limit any possible damage the leaching of cerium from materials.

REFERENCES

1. **Aguirre, T., G. Matthijs, W. Robberecht, P. Tilkin, and J. J. Cassiman.** 1999. Mutational analysis of the Cu/Zn superoxide dismutase gene in 23 familial and 69 sporadic cases of amyotrophic lateral sclerosis in Belgium. Eur J Hum Genet **7:**599-602.
2. **Arner, E. S., and A. Holmgren.** 2000. Physiological functions of thioredoxin and thioredoxin reductase. Eur J Biochem **267:**6102-9.
3. **Bailey, D. M., S. Raman, J. McEneny, I. S. Young, K. L. Parham, D. A. Hullin, B. Davies, G. McKeeman, J. M. McCord, and M. H. Lewis.** 2006. Vitamin C prophylaxis promotes oxidative lipid damage during surgical ischemia-reperfusion. Free Radic Biol Med **40:**591-600.
4. **Berg, D., C. Grote, W. D. Rausch, M. Maurer, W. Wesemann, P. Riederer, and G. Becker.** 1999. Iron accumulation in the substantia nigra in rats visualized by ultrasound. Ultrasound Med Biol **25:**901-4.
5. **Borthiry, G. R., W. E. Antholine, B. Kalyanaraman, J. M. Myers, and C. R. Myers.** 2007. Reduction of hexavalent chromium by human cytochrome b5: generation of hydroxyl radical and superoxide. Free Radic Biol Med **42:**738-55; discussion 735-7.
6. **Campbell, C. T., and C. H. Peden.** 2005. Chemistry. Oxygen vacancies and catalysis on ceria surfaces. Science **309:**713-4.

7. **Childs, R. E., and W. G. Bardsley.** 1975. The steady-state kinetics of peroxidase with 2,2'-azino-di-(3-ethyl-benzthiazoline-6-sulphonic acid) as chromogen. Biochem J **145:**93-103.

8. **Coggins, M. P., and K. D. Bloch.** 2007. Nitric oxide in the pulmonary vasculature. Arterioscler Thromb Vasc Biol **27:**1877-85.

9. **Crouch, P. J., A. R. White, and A. I. Bush.** 2007. The modulation of metal bio-availability as a therapeutic strategy for the treatment of Alzheimer's disease. Febs J **274:**3775-83.

10. **Das, M., S. Patil, N. Bhargava, J. F. Kang, L. M. Riedel, S. Seal, and J. J. Hickman.** 2007. Auto-catalytic ceria nanoparticles offer neuroprotection to adult rat spinal cord neurons. Biomaterials **28:**1918-25.

11. **Frejaville, C., H. Karoui, B. Tuccio, F. Le Moigne, M. Culcasi, S. Pietri, R. Lauricella, and P. Tordo.** 1995. 5-(Diethoxyphosphoryl)-5-methyl-1-pyrroline N-oxide: a new efficient phosphorylated nitrone for the in vitro and in vivo spin trapping of oxygen-centered radicals. J Med Chem **38:**258-65.

12. **Fridovich, I.** 2004. Mitochondria: are they the seat of senescence? Aging Cell **3:**13-6.

13. **Fridovich, I.** 1970. Quantitative aspects of the production of superoxide anion radical by milk xanthine oxidase. J Biol Chem **245:**4053-7.

14. **Garnett, M. C., and P. Kallinteri.** 2006. Nanomedicines and nanotoxicology: some physiological principles. Occup Med (Lond) **56:**307-11.

15. **Hu, Z. Y., S. Haneklaus, G. Sparovek, and E. Schnug.** 2006. Rare earth elements in soils. Communications in Soil Science and Plant Analysis **37:**1381-1420.

16. **Imlay, J. A., S. M. Chin, and S. Linn.** 1988. Toxic DNA damage by hydrogen peroxide through the Fenton reaction in vivo and in vitro. Science **240:**640-2.

17. **Jasinski, P., T. Suzuki, and H. U. Anderson.** 2003. Nanocrystalline undoped ceria oxygen sensor. Sensors and Actuators B-Chemical **95:**73-77.

18. **Jezek, P., and L. Hlavata.** 2005. Mitochondria in homeostasis of reactive oxygen species in cell, tissues, and organism. Int J Biochem Cell Biol **37:**2478-503.

19. **Jiang, H., Z. Luan, J. Wang, and J. Xie.** 2006. Neuroprotective effects of iron chelator Desferal on dopaminergic neurons in the substantia nigra of rats with iron-overload. Neurochem Int **49:**605-9.

20. **Kaur, D., F. Yantiri, S. Rajagopalan, J. Kumar, J. Q. Mo, R. Boonplueang, V. Viswanath, R. Jacobs, L. Yang, M. F. Beal, D. DiMonte, I. Volitaskis, L. Ellerby, R. A. Cherny, A. I. Bush, and J. K. Andersen.** 2003. Genetic or pharmacological iron chelation prevents MPTP-induced neurotoxicity in vivo: a novel therapy for Parkinson's disease. Neuron **37:**899-909.

21. **Koorts, A. M., and M. Viljoen.** 2007. Ferritin and ferritin isoforms I: Structure-function relationships, synthesis, degradation and secretion. Arch Physiol Biochem **113:**30-54.

22. **Korsvik, C., S. Patil, S. Seal, and W. T. Self.** 2007. Superoxide dismutase mimetic properties exhibited by vacancy engineered ceria nanoparticles. Chem Commun (Camb)**:**1056-8.

23. **Kuiry, S. C., S. D. Patil, S. Deshpande, and S. Seal.** 2005. Spontaneous self-assembly of cerium oxide nanoparticles to nanorods through supraaggregate formation. J Phys Chem B Condens Matter Mater Surf Interfaces Biophys **109:**6936-9.

24. **Kuruvilla, L., and C. C. Kartha.** 2006. Cerium depresses endocardial endothelial cell-mediated proliferation of cardiac fibroblasts. Biol Trace Elem Res **114:**85-92.

25. **Lam, C. W., J. T. James, R. McCluskey, and R. L. Hunter.** 2004. Pulmonary toxicity of single-wall carbon nanotubes in mice 7 and 90 days after intratracheal instillation. Toxicol Sci **77:**126-34.

26. **Liochev, S. I., and I. Fridovich.** 2003. Mutant Cu,Zn superoxide dismutases and familial amyotrophic lateral sclerosis: evaluation of oxidative hypotheses. Free Radic Biol Med **34:**1383-9.

27. **Magrez, A., S. Kasas, V. Salicio, N. Pasquier, J. W. Seo, M. Celio, S. Catsicas, B. Schwaller, and L. Forro.** 2006. Cellular toxicity of carbon-based nanomaterials. Nano Lett **6:**1121-5.

28. **McCord, J. M., and I. Fridovich.** 1969. Superoxide dismutase. An enzymic function for erythrocuprein (hemocuprein). J Biol Chem **244:**6049-55.

29. **Medalia, A., and B. Byrne.** 1951. Spectrophotometric Determination of of Cerium (IV). Anal. Chem. **23:**453-456.

30. **Mehta, A., S. Patil, H. Bang, H. J. Cho, and S. Seal.** 2007. A novel multivalent nanomaterial based hydrogen peroxide sensor. Sensors and Actuators a-Physical **134:**146-151.

31. **Nikolaou, K.** 1999. Emissions reduction of high and low polluting new technology vehicles equipped with a CeO2 catalytic system. Sci Total Environ **235:**71-6.

32. **Niu, J., A. Azfer, L. M. Rogers, X. Wang, and P. E. Kolattukudy.** 2007. Cardioprotective effects of cerium oxide nanoparticles in a transgenic murine model of cardiomyopathy. Cardiovasc Res **73:**549-59.

33. **Park, S., X. You, and J. A. Imlay.** 2005. Substantial DNA damage from submicromolar intracellular hydrogen peroxide detected in Hpx- mutants of Escherichia coli. Proc Natl Acad Sci U S A **102:**9317-22.

34. **Pastor, N., H. Weinstein, E. Jamison, and M. Brenowitz.** 2000. A detailed interpretation of OH radical footprints in a TBP-DNA complex reveals the role of dynamics in the mechanism of sequence-specific binding. J Mol Biol **304:**55-68.

35. **Preeta, R., and R. R. Nair.** 1999. Stimulation of cardiac fibroblast proliferation by cerium: a superoxide anion-mediated response. Journal of Molecular and Cellular Cardiology **31:**1573-1580.

36. **Purdy, D., S. Cawthraw, J. H. Dickinson, D. G. Newell, and S. F. Park.** 1999. Generation of a superoxide dismutase (SOD)-deficient mutant of Campylobacter coli: evidence for the significance of SOD in Campylobacter survival and colonization. Appl Environ Microbiol **65:**2540-6.

37. **Qian, S. Y., and G. R. Buettner.** 1999. Iron and dioxygen chemistry is an important route to initiation of biological free radical oxidations: an electron paramagnetic resonance spin trapping study. Free Radic Biol Med **26:**1447-56.

38. **Rae, T. D., P. J. Schmidt, R. A. Pufahl, V. C. Culotta, and T. V. O'Halloran.** 1999. Undetectable intracellular free copper: the requirement of a copper chaperone for superoxide dismutase. Science **284:**805-8.

39. **Ramos, C. L., S. Pou, and G. M. Rosen.** 1995. Effect of anti-inflammatory drugs on myeloperoxidase-dependent hydroxyl radical generation by human neutrophils. Biochem Pharmacol **49:**1079-84.

40. **Sagach, V. F., M. Scrosati, J. Fielding, G. Rossoni, C. Galli, and F. Visioli.** 2002. The water-soluble vitamin E analogue Trolox protects against ischaemia/reperfusion damage in vitro and ex vivo. A comparison with vitamin E. Pharmacol Res **45:**435-9.

41. **Sayle, T. X., S. C. Parker, and D. C. Sayle.** 2005. Oxidising CO to CO2 using ceria nanoparticles. Phys Chem Chem Phys **7:**2936-41.

42. **Schubert, D., R. Dargusch, J. Raitano, and S. W. Chan.** 2006. Cerium and yttrium oxide nanoparticles are neuroprotective. Biochem Biophys Res Commun **342:**86-91.

43. **Sigler, P. B., and B. J. Masters.** 1957. The Hydrogen Peroxide-induced Ce*(III)-Ce(IV) Exchange System. J. Am. Chem. Soc. **79:**6353-6357.

44. **Sugden, K. D., R. D. Geer, and S. J. Rogers.** 1992. Oxygen radical-mediated DNA damage by redox-active Cr(III) complexes. Biochemistry **31:**11626-31.

45. **Sugiura, M.** 2003. Oxygen storage materials for automotive catalysts: ceria-zirconia solid solutions. Catalysis Surveys from Asia **7:**77-87.

46. **Swindle, E. J., J. A. Hunt, and J. W. Coleman.** 2002. A comparison of reactive oxygen species generation by rat peritoneal macrophages and mast cells using the highly sensitive real-time chemiluminescent probe pholasin: inhibition of antigen-induced mast cell degranulation by macrophage-derived hydrogen peroxide. J Immunol **169:**5866-73.

47. **Tarnuzzer, R. W., J. Colon, S. Patil, and S. Seal.** 2005. Vacancy engineered ceria nanostructures for protection from radiation-induced cellular damage. Nano Lett **5:**2573-7.

48. **Teeguarden, J. G., P. M. Hinderliter, G. Orr, B. D. Thrall, and J. G. Pounds.** 2007. Particokinetics in vitro: dosimetry considerations for in vitro nanoparticle toxicity assessments. Toxicol Sci **95:**300-12.

49. **Touyz, R. M.** 2004. Reactive oxygen species, vascular oxidative stress, and redox signaling in hypertension: what is the clinical significance? Hypertension **44:**248-52.

50. **Toyokuni, S.** 1996. Iron-induced carcinogenesis: the role of redox regulation. Free Radic Biol Med **20:**553-66.

51. **Valko, M., C. J. Rhodes, J. Moncol, M. Izakovic, and M. Mazur.** 2006. Free radicals, metals and antioxidants in oxidative stress-induced cancer. Chem Biol Interact **160:**1-40.

52. **Xu, X., W. Zhu, Z. Wang, and G. J. Witkamp.** 2002. Distributions of rare earths and heavy metals in field-grown maize after application of rare earth-containing fertilizer. Sci Total Environ **293:**97-105.

53. **Yeldandi, A. V., M. S. Rao, and J. K. Reddy.** 2000. Hydrogen peroxide generation in peroxisome proliferator-induced oncogenesis. Mutat Res **448:**159-77.

54. **Yim, M. B., P. B. Chock, and E. R. Stadtman.** 1993. Enzyme function of copper, zinc superoxide dismutase as a free radical generator. J Biol Chem **268:**4099-105.

55. **Yu, L., Y. Dai, Z. Yuan, and J. Li.** 2007. Effects of rare earth elements on telomerase activity and apoptosis of human peripheral blood mononuclear cells. Biol Trace Elem Res **116:**53-9.

56. **Zhu, X., B. Su, X. Wang, M. A. Smith, and G. Perry.** 2007. Causes of oxidative stress in Alzheimer disease. Cell Mol Life Sci **64:**2202-10.